NATIONAL ADVISORY COMMITTEE FOR AERONAUTICS

TECHNICAL NOTE 4160

THERMAL FATIGUE OF DUCTILE MATERIALS

I - EFFECT OF VARIATIONS IN THE TEMPERATURE CYCLE ON THE

THERMAL-FATIGUE LIFE OF S-816 AND INCONEL 550

By Francis J. Clauss and James W. Freeman

Lewis Flight Propulsion Laboratory
Cleveland, Ohio

Washington

September 1958

NATIONAL ADVISORY COMMITTEE FOR AERONAUTICS

4669

TECHNICAL NOTE 4160

THERMAL FATIGUE OF DUCTILE MATERIALS

I - EFFECT OF VARIATIONS IN THE TEMPERATURE CYCLE ON THE

THERMAL-FATIGUE LIFE OF S-816 AND INCONEL 550[*]

By Francis J. Clauss and James W. Freeman

SUMMARY

An experimental study was made of the effect of the following factors on the life of two ductile alloys (S-816 and Inconel 550) under high-temperature thermal-fatigue conditions:

(1) The maximum cycle temperature, T_{max}

(2) The temperature difference of cycling, $\Delta T = T_{max} - T_{min}$

(3) The cyclic time of exposure at the maximum cycle temperature, t at T_{max}

(4) The cyclic plastic strain, ε_p.

Tensile specimens of S-816 and Inconel 550 were alternately heated and cooled while constrained in a manner that prevented their free axial expansion and contraction, and the number of cycles to fracture was determined. Hardness measurements and microstructural studies were made.

For the materials and test conditions studied, the following conclusions were drawn:

The number of cycles to failure was more sensitive to changes in the maximum cycle temperature than to changes in the temperature difference.

---

[*]The information presented in this report was offered by Dr. F. J. Clauss as a thesis in partial fulfillment of the requirements for the degree of Doctor of Philosophy in Metallurgical Engineering, University of Michigan, Ann Arbor, Michigan, June 1957. Professor James W. Freeman was chairman of Dr. Clauss' doctoral committee and is also a consultant to the Lewis Flight Propulsion Laboratory.

INTRODUCTION

Thermal fatigue is the process by which a material ultimately fractures after being repeatedly heated and cooled without being allowed to expand and contract freely. Though thermal-fatigue failures are by no means a new problem, the trends in modern technology to higher temperatures and cyclic operations have increased their occurrence and damaging effects. Numerous examples have been discussed in the literature, for example, power generating plants (refs. 1 and 2), petroleum refineries (refs. 3, 4, and 5), turbojet engines (refs. 6 to 10), and nuclear reactors (ref. 11).

Considering its importance, there is very little fundamental information available on thermal fatigue in ductile materials. Mathematical analyses have been largely confined to brittle materials or to idealized conditions in ductile ones. Laboratory results on the relative merits of real materials in thermal fatigue have not always been consistent, nor have attempts to correlate them with service performance always been successful.

A program of fundamental research on the thermal-fatigue process in ductile materials has been conducted at the Lewis laboratory of the National Advisory Committee for Aeronautics, and the results are presented here and in reference 12. The present report reviews the literature on thermal fatigue and presents results on the effects of various test conditions on the number of cycles to complete failure. Reference 12 deals with changes in the material properties that occur prior to failure as a result of various amounts of exposure to thermal-fatigue conditions, and it also extends existing theories of mechanical fatigue and creep rupture to explain the behavior of ductile alloys during thermal fatigue.

The specific purposes of the present experimental investigation were to study the effects of the following conditions on the thermal-fatigue life:

(1) The maximum cycle temperature, T_{max}

(2) The temperature difference of cycling, $\Delta T = T_{max} - T_{min}$

(3) The cyclic time of exposure at the maximum cycle temperature, t at T_{max}

(4) The cyclic plastic strain, ε_p (which, of course, depends on ΔT and the other test conditions).

In the experimental part of this study, tensile-type specimens of S-816 and Inconel 550 alloys were heated and cooled through various temperature cycles while they were constrained from expanding and contracting

axially. These two alloys are both precipitation-hardening "superalloys" used in turbojet engines. The maximum cycle temperatures to which these alloys were heated ranged from $1150°$ to $1600°$ F; the minimum cycle temperature was $200°$ F in most cases, although it ranged as high as $500°$ F. The test cycle that was generally followed consisted of the following: (1) heat 30 seconds to T_{max}, (2) hold 15 seconds at T_{max}, (3) cool 30 seconds to T_{min}, (4) hold 15 seconds at T_{min}, and then repeat the cycle. For some tests, the time of holding at T_{max} was increased to 60 seconds. The number of cycles to fracture, changes in hardness, and microstructural behavior were studied as a function of the conditions of temperature cycling.

PRELIMINARY CONSIDERATIONS AND LITERATURE SURVEY

Basic Concepts

Thermal stress. - When a solid is heated or cooled nonuniformly, the various sections tend to expand or contract in different amounts. The same is true if the temperature is changed uniformly throughout a body composed of several materials with different rates of thermal expansion. To enable such bodies to remain continuous, systems of thermal strains and associated stresses are set up internally. The magnitude of the thermal stresses depends on: The temperature distribution within the body, the properties of the material, and the degree of constraint, which is imposed by the continuity of the body and by external boundary conditions.

Thermal shock. - Thermal shock means either sudden heating or cooling. The thermal stresses caused by thermal shock are generally greater than those that occur during slow heating or cooling for two reasons: The transient temperature distributions produced within the body during sudden heating or cooling are more severe, and also the thermal stresses do not have time to be relieved by relaxation during sudden heating or cooling.

When the thermal stress at some point in the body exceeds the fracture strength of the material, the body will fracture at that point. Failure in a single cycle of heating or cooling occurs when the body cannot deform plastically to relieve the thermal stress, and this usually implies thermal-shock conditions, a high degree of constraint, and/or a brittle material.

Thermal fatigue. - Thermal fatigue refers to the process by which failure occurs after a repeated number of cycles of thermal stressing. This process is much more complex than when a failure occurs on the first cycle. It includes certain elements present in normal mechanical fatigue at low temperatures, such as cyclic plastic deformation in tension and compression that ultimately exhausts the ductility of the material and causes a fatigue crack. It also includes certain elements of the normal creep-rupture process at high temperatures. Thus, while the material is at the high temperature of the cycle, annealing may occur to relieve the strain-hardening due to reversed plastic deformation, or secondary phases may precipitate along slip lines and cause additional hardening. The structural changes that occur depend on the material, the strain, and the temperature involved, and they may change the strength and ductility so much that the material will fracture from causes other than thermal fatigue. On the other hand, long before the material cracks or fractures, it may warp or distort to a degree that exceeds the dimensional tolerances.

Thermal-Stress Tests

Material evaluation. - Laboratory tests for measuring the resistance of materials to thermal stresses are not yet standardized and often produce results that are contradictory with one another and with actual service records.

In general, two methods of testing are used:[1]

First specimens are subjected to varying temperature changes, and the minimum temperature change that will cause the specimen to fail in a single cycle under otherwise specified conditions is measured.

Next, specimens are repeatedly subjected to the same temperature cycle, and the number of cycles that the specimens survive before failing under the specified conditions is measured.

In both of these tests, failure is usually defined either as visible cracking at the surface or as actual fracture across the cross section. The first type of test is usually confined to brittle materials. The second type is more common with ductile materials, which seldom fail in

---

[1]A third type of test, which will not be discussed, is one that has been standardized by the American Society for Testing Materials for classifying the resistance of refractory bricks or block to spalling. Spalling involves a weight loss due to flaking of the surface layer or to chipping of the corners of the brick, and the ASTM test classifies the bricks on the basis of the percentage weight loss after a specific spalling test.

a single cycle because of their ability to deform and relieve the stresses. A variation of these two tests (accelerated life test) is also used in which the test is run for a limited number of cycles at a fixed temperature change and, if the specimen does not fail, the temperature change is raised and the test continued in the same manner until failure does occur.

Literature review. - The results of an early German study of the resistance of high-temperature alloys to repeated thermal shock are described in an English survey in reference 13. Wedge-shaped specimens of various materials were heated in a flame for 1 minute and then cooled in still air for 3 minutes. The specimens were cycled to two temperatures: one at 650° to 700° C (1202° to 1292° F), the other at 850° to 900° C (1562° to 1652° F). Specimens failed either by severe distortion of the edge or by the formation of cracks. These tests demonstrated the following:

(1) Excessive distortion, as well as cracking, can limit the serviceability under thermal-fatigue conditions.

(2) The number of cycles to failure falls off very rapidly as the temperature difference (or maximum cycle temperature) is increased.

(3) The relative merit of several materials can change with the test conditions. Therefore, tests for rating materials must closely approach the conditions of the intended service, or the results can be misleading.

(4) No clear relation exists between the resistance to thermal shock and such material properties as tensile or creep-rupture strength.

Tests were conducted at the NACA (ref. 14) to measure the resistance of six cast high-temperature alloys (S-816, S-590, HS-21, 422-19, X-40, and Stellite 6) to thermal shock. Specimens were cast in the form of wedges and were heated to a uniform temperature of 1750° F for 1 hour and then quenched in water along a 1/32-inch wide edge. When the specimens were cool, they were removed from the quenching apparatus, the oxide films were carefully removed from the narrow edges, and these edges were microscopically examined for cracks. Failure was arbitrarily defined as the presence of an opening across the entire width of the quenched edge.

No correlation was found between the thermal properties (coefficient of linear expansion, thermal conductivity, and specific heat) and the resistance of the alloys to thermal cracking. Since the thermal properties of the six alloys did not vary over a wide range, whereas the number of cycles to failure varied by a factor of more than 10, the investigation demonstrated that materials with similar thermal properties can have widely different resistances to thermal cracking.

Besides cracking, the specimens also warped so that the quenched edges bowed. The amount of bowing increased with the number of cycles; the rate of bowing decreased as the number of cycles increased. Although the rates of bowing were different for the alloys, the greater the number of cycles to failure, the greater was the amount of bowing at failure.

Tests similar to the NACA test in which wedge- or triangular-shaped specimens were heated and/or cooled along one edge have been used by many other investigators. One manufacturer, for example, has conducted a thermal-shock test which involved repeated cycles of heating the edge of a triangular-shaped sample in a flame to a maximum temperature of 1800° F and sudden cooling of this edge to 800° F in a blast of compressed air (ref. 15). Failure occurred when a crack had progressed completely across the 1/32-inch edge of the specimen.

The data obtained in this study showed that cast HS-21 and X-40 were superior to cast S-816, whereas they were both inferior to cast S-816 in the tests cited in reference 14. This discrepancy may have been due to differences in the lots of material or in the test conditions.

The significance of the differences between the alloys in the thermal-shock test as related to actual service behavior was not determined in the commercial study, nor were attempts to correlate thermal shock resistance with other common properties successful.

L. F. Coffin, Jr. (refs. 16 to 19) has presented a most interesting and detailed study of the thermal fatigue of thin tubular specimens of type 347 stainless steel. These specimens were constrained longitudinally by being gripped in a rig that clamped on to flanges at their ends. In most cases, the specimens were initially stress-free and clamped at the upper temperature limit. (Coffin found no difference in the thermal-fatigue life regardless of whether the specimens were clamped at the upper or the lower temperature.) The effect of the temperature difference of cycling was studied by varying ΔT from 200° to 500° C while holding the mean temperature constant at 350° C; that is, T_{max}/T_{min} varied from 450°/250° C to 600°/100° C (842°/482° F to 1112°/212° F, respectively). The average temperature was held constant in an effort to minimize the effect of temperature on the material and to measure only the effect of varying amounts of thermal strain associated with the various ΔT values. The frequency of cycling was 4 cycles per minute, which is unusually fast for thermal-fatigue tests, and failure was defined as a complete or nearly complete fracture of the specimen. Under these conditions, the thermal-fatigue life of annealed specimens dropped from about 40,000 to 1800 cycles as the ΔT was increased from 200° to 500° C.

The effect of cold-working was studied by prestraining specimens in tension or torsion. At high values of ΔT, prior cold work reduced the

life; for example, at a ΔT of 400° C, a 360° twist in the specimen
reduced its life to 650 cycles, as compared with 3800 cycles for the
annealed material. As the ΔT was reduced, the damaging effect was
less, and in several cases the cold-worked material became better than
the annealed material at low ΔT values; thus, the curve for a 360° pre-
twist crossed that for annealed material at a ΔT of about 300° C.
Coffin found that the kind or prior cold work was not important in thermal
cycling. Specimens cold-worked by torsion or by tension withstood the
same number of cycles of thermal stressing, so long as both were worked
to the same amount of effective strain.

Coffin also studied the effect of mean temperature on thermal fatigue
by testing specimens at mean temperatures of 250°, 350°, and 450° C while
maintaining the ΔT at about 300° C. Because of the slight change in
the expansion coefficient with temperature, the free thermal expansion
for a ΔT of 300° C was greater at a mean temperature of 450° C than at
the lower mean temperatures, and the ΔT values were therefore adjusted
slightly to maintain constant strain amplitudes. An increase in mean
temperature under these conditions decreased the thermal-fatigue life
from about 15,000 cycles at a mean temperature of 250° C to 8000 cycles
at 450° C.

In another series of tests cycled between 200° and 500° C, the time
that the specimens were at 500° C was varied. While there was consider-
able scatter in these results, increasing the hold time from 6 to 180
seconds appeared to decrease the number of cycles to failure from about
10,000 to 7000 with a possible minimum for a hold time of 60 seconds.
Coffin felt that, from a practical point of view, the decrease in the
number of cycles to failure with increased hold times was small and
pointed out that the life was actually increased if the total elapsed
time of the tests was used rather than the number of cycles.

Efforts to correlate and explain experimental results from thermal-
fatigue tests have emphasized the similarity to ordinary mechanical fa-
tigue and the role of strain-hardening. The basic postulate of these
efforts seems to be that failure occurs when the ductility of the material
has been exhausted so that it is no longer able to absorb the reversed
deformation.

As a first estimate, the sum of the absolute values of the tensile
and compressive strains during each cycle multiplied by the number of
cycles to failure might be thought to equal the amount of strain at
failure measured in a simple tensile or compression test. Experimentally
this is not true and, in fact, even the summation of only the tensile
components of plastic flow during cycling is greater than the ductility
of the initial material in the conventional tensile test. Repeated
increments of plastic flow thus appear to improve the subsequent behavior.

Experiments also show that the summation of the components of tensile and compressive flow during cycling varies with the test conditions, and that the greater the number of cycles to failure, the greater is this summation. S. S. Manson (ref. 20) proposed the following relation in 1952 to express this

$$N_f = K\epsilon_p^{-n} \tag{1}$$

where

N_f = number of cycles to failure

ϵ_p = plastic strain per cycle

K and n = constants

Manson (ref. 20) applied this relation to mechanical-fatigue data on 24ST aluminum at room temperature (ref. 21) and estimated that the value of the exponent in equation (1) should be about 3. Later analysis of the same data showed that the exponent was more nearly 2 (ref. 19). The important point demonstrated by these analyses was that the number of cycles to failure appeared to bear a simple relation to the amount of strain per cycle in mechanical fatigue. Manson (ref. 20) further suggested that this relation might prove valuable in thermal fatigue, and it was used to illustrate the drastic reduction in the number of cycles to failure that might be expected from increasing the ΔT of cycling. For example, consider a bar with fixed ends that is made of an ideally plastic material with the following properties, independent of temperature:

Coefficient of thermal expansion, α, in./in./°F . . . . 10×10^{-6}
Modulus of elasticity, E, psi . . . . 30×10^6
Yield strength in tension and compression, σ^*, psi 90,000

Such a material would deform plastically when the strain exceeded 0.003 inch per inch. It would undergo reversed plastic deformation on cycling when $\alpha\Delta T \geq 2(0.003)$; this makes $\Delta T \geq 600°$ F. The plastic strain per half cycle ϵ_p would then be given as

$$\epsilon_p = 10\times10^{-6} \Delta T - 0.006 \tag{2}$$

The number of cycles to failure, relative to 1000 cycles at a ΔT of 800° F, would then be as follows:

4669

$\Delta T,$ $^\circ F$	$\epsilon_p,$ in./in.	ϵ_p	$N_f = K\epsilon_p^{-2}$ (Relative to $N = 1000$ at $\Delta T = 800^\circ$ F)
600	0.000	0	∞
800	.002	4×10^{-9}	1000
1000	.004	16×10^{-9}	250
1200	.006	36×10^{-9}	111
1400	.008	64×10^{-9}	62
1600	.010	100×10^{-9}	40
1800	.012	144×10^{-9}	28

Thus, the analysis predicts that the number of cycles to failure should drop off rapidly as the temperature change is increased, as was observed experimentally in the tests quoted in reference 13.

Going from an ideally plastic material to a real material introduces a number of changes in the behavior from this ideal model. For example, the following must be considered:

(1) Strain-hardening, by which prior deformation increases the yield strength and reduces the amount of reversed plastic flow

(2) The Bauschinger effect, by which plastic flow in one direction reduces the stress at which plastic flow occurs in the opposite direction

(3) The temperature dependence of the mechanical properties

(4) The temperature dependence of the thermal properties

(5) The time dependence of the mechanical properties, as the effect of strain rate on the yield point

(6) Time effects such as creep and stress-relaxation, which become especially important at high temperatures

Microstructural changes that alter properties may also occur during cycling, particularly if the temperatures are high. These will increase the list of factors to be considered as follows:

(7) Recovery, recrystallization, and grain growth

(8) Matrix transformations

(9) Aging, precipitation-hardening, overaging, and spheroidization

(10) Anisotropic effects

(11) Corrosion

CE-2

(12) Formation of cracks, which can reduce the load-bearing area or
     act as stress-raisers

Finally, the practical case may add the following changes to the
simple bar model described:

(13) Nonuniformity of temperature over the cross section and length
     of the specimen

(14) Nonuniformity of cross-sectional area over the length of the
     specimen

(15) Stress concentrations

(16) Incomplete constraint due to yielding of the supports

(17) Size effects

Despite these limitations, Coffin (refs. 16 to 18) had considerable
success in applying equation (1) to his experimental results on thermal-
fatigue failures. Thus, Coffin correlated his results on the thermal
cycling of annealed-type 347 stainless steel at a constant mean temperature
of 350° C by the relation

$$N_f^{1/2} \epsilon_p = 0.36 \tag{3}$$

or, its equivalent form

$$N_f = 0.1296 \, \epsilon_p^{-2} \tag{4}$$

When the specimens were strain cycled at a constant temperature of 350° C
(i.e., the same as the mean temperature of the thermal cycling tests),
the relation was

$$N_f^{0.43} \epsilon_p = 0.28 \tag{5}$$

or

$$N_f = 0.05177 \, \epsilon_p^{-2.326} \tag{6}$$

The quantity ϵ_p in these relations is the plastic-strain change
per cycle. Since this changes during cycling because of strain-hardening
or softening, Coffin used a calculated plastic-strain change at one-half
the number of cycles for failure. The calculation was based on the
relation

$$\epsilon_{thermal} + \epsilon_{elastic} + \epsilon_{inelastic} = \epsilon_{net} = 0 \tag{7}$$

which states: (1) the net strain of the tubular specimens was zero,
since the ends were held fixed (or very nearly so) in a gripping device,

and (2) the free thermal expansion or contraction was offset by an equal
and opposite flow made up by an elastic and a plastic component. The
quantity $\epsilon_{thermal}$ could be determined either by measuring the free
expansion or contraction that occurred when the specimen was unclamped or
by calculating it as equal to $\alpha\Delta T$ where α is the average coefficient
of thermal expansion. Actually, as Coffin points out, the quantity $\alpha\Delta T$
was not exactly equal to the thermal strain because of longitudinal heat
transfer, which caused the ends of the specimens to be colder than the
middles.

The elastic strain $\epsilon_{elastic}$ was determined from the stress change
per cycle at one-half the number of cycles to failure and from the modulus
of elasticity. The constrained expansion and contraction of the specimens
caused a very slight strain in the massive bars that connected the end
plates holding the specimens. The strain in the bars was measured by
SR-4 strain gages cemented to them and was converted to stress by multi-
plying by the modulus of elasticity of the bar material. Multiplying
this stress by the ratio of the areas of the bars and specimen gave the
stress in the specimen. The stress in the specimen was then divided by
its modulus of elasticity to give $\epsilon_{elastic}$. The modulus of elasticity
would, of course, have to be an average modulus for the temperatures
involved, and the strain would be an average strain over the length of
the specimen. The values of $\epsilon_{thermal}$ and $\epsilon_{elastic}$ were then inserted
into equation (9) to give $\epsilon_{plastic}$. While the procedure involves some
simplifying assumptions, the final correlations between N_f and ϵ_p
appear remarkably good.

The success of equation (1), as well as other experimental observa-
tions, led Coffin to believe that the strain change is the dominant factor
controlling thermal fatigue and that temperature effects are not so
important. He pointed out, however, that differences may be encountered
under temperature conditions where phase changes, marked strain-aging, or
anisotropic effects occur. Coffin added that "Except for the possibility
of some transformation of gamma-iron to alpha-iron with extreme cold work
none of the above effects can occur for type-347 stainless steel. It
appears then that temperature cycling has only a secondary effect on the
fundamental aspects of the problem (ref. 17)." As added proof, Coffin
points out that there is no change in the stress-strain behavior of an
annealed-type 347 stainless steel if it is thermally cycled without con-
straint for 10,000 cycles between 200° and 500° C (i.e., if it is exposed
to the temperature conditions without straining). However, structural
changes are influenced by both temperature and strain; changes that do
not occur under temperature or strain alone may occur when both are pre-
sent. Also, the drop in life with the temperature level of testing at
constant strain amplitude (see p. 7) challenges the hypothesis that tem-
perature effects are not important.

In summary, although plastic deformation and strain-hardening appear
to be well established as important factors in thermal fatigue, the im-
portance of the temperature level of cycling remains undefined.   In view
of the tremendous effect that temperature has on the properties of mate-
rials, it is reasonable to expect that its role in thermal fatigue is
important.   In addition, time becomes a factor in the behavior of metals
at high temperatures, and the frequency of cycling would therefore be
expected to affect the number of cycles to failure.   If these factors
are important, the correlations of the number of cycles to failure with
the amount of plastic deformation per cycle may need to be modified by
including the effects of both temperature and time in order to have gen-
eral applicability.   Information on these effects should also aid in
understanding the mechanism of thermal fatigue.

EQUIPMENT AND PROCEDURE

Equipment

The equipment and procedure minimized the thermal stresses in other
than the axial direction of the specimens.   Figure 1 shows the specimen
design.   The center section was heated and cooled through the desired
temperature cycle by passing high-amperage - low-voltage current through
it by means of water-cooled, copper leads that attached to the adjacent
shoulders.   The specimens were constrained from expanding and contracting
axially by gripping them tightly about the shoulders at opposite ends.
The advantages which this type of specimen and procedure have over earlier
thermal-fatigue tests are that the thermal stresses and strains are uni-
axial and can be measured and that a specimen can be removed from the
gripping block prior to failure and, subsequently, threaded on the oppo-
site shoulders and tested in stress-rupture (ref. 12).

The block for gripping the specimens is shown in figure 2.   This was
a 7-inch square by 3-inch thick steel block with a 2.50-inch-diameter
hole drilled out through the center of the faces and a 0.50-inch-diameter
hole running from top to bottom.   The block was split into two halves
that were fastened together on the specimens by four bolts.   Tightening
the bolts caused the block to grip the specimen tightly on the end
shoulders.   The block was massive enough and the frictional gripping
force was firm enough so that there was no measurable movement of the
end shoulders of the specimens during constrained thermal cycling.   The
specimen and block were electrically insulated from each other by 0.002-
to 0.004-inch paper.

A single chromel-alumel thermocouple was spotwelded to the center of
the test section to measure temperatures, and the temperatures were re-
corded continuously on a Brown recording potentiometer.   Small-diameter
thermocouple wires were used to minimize heat conduction from the

specimen. Tests indicated that spot-welding the thermocouples on the specimens did not interfere with the results. Figure 3 shows the thermocouple wires spotted on a specimen that had been removed from thermal cycling before failure. Note that the manner of attaching the thermocouple had no apparent effect on the material other than causing a very small amount of recrystallization immediately below the couple.

The test section of a specimen was raised to the desired temperature by electric resistance heating. During cooling, the power input was reduced and heat was removed from the test section by conduction through the shoulders to the water-cooled, copper leads and by transfer to still air. Both the copper leads and the gripping block were included in the water-cooling circuit. Because the shoulders of the specimens were maintained at relatively low temperatures, the temperature was not uniform along the length of the test sections, as shown in the temperature profiles in figure 4. Both S-816 and Inconel 550 showed the same temperature profiles, as determined from thermocouples spotwelded at various points along the lengths of the test sections of several specimens. The cycle temperatures reported in this study are those at the center of the test section.

Suitable electric controls were provided so that the specimens could be heated and cooled automatically between the desired temperatures and in the desired times.

The expansion and contraction of the test section caused the shoulders adjacent to it to deflect slightly. The amount of this movement was measured by a mechanical strain gage with knife edges that rode on the shoulders, as shown in figure 2. A mirror mounted at the other end of the strain gage reflected the readings from a graduated scale into a telescope placed next to the scale and several feet from the specimen. As the shoulders of the test section moved, the mirror rotated, and the amount of movement was measured by the change in the scale readings received at the telescope. The lever arms and scale-to-mirror distance were such that the movement of the shoulder was magnified about 200 times. The movement of the shoulders corresponded to the change in the total length of the test section, and this change was not uniform because of the temperature gradient along the axis of the test section.

For some of the calculations, it was necessary to know the amount of free expansion and contraction in the shoulders adjacent to the test section as the specimen was thermally cycled. This was determined by using a dial gage at the loose end of the specimen to measure the total movement of the specimen when it was thermally cycled without constraint. Subtracting the movement in the test section (as measured by the strain gage) from this total movement gave the free expansion or contraction of the shoulders. Since the temperature of the large shoulders at the opposite ends of the specimens was unchanged during thermal cycling, this shoulder movement was confined to the two shoulders immediately adjacent to the test section.

Figure 5 consists of photographs of the actual equipment.

Materials

Two materials were studied, namely, S-816 and Inconel 550 alloys. These are both high-temperature superalloys that are used mainly at temperatures on the order of 1350° to 1500° F. Of the two alloys, S-816 is weaker at these temperatures but has more ductility than Inconel 550. S-816 is a cobalt-base alloy, while Inconel 550 is nickel base; their nominal compositions are as follows:

Alloy	Percent by weight									
	C	Cr	Ni	Co	Mo	W	Nb	Ti	Al	Fe
S-816	0.4	20.0	20.0	Bal.	4.0	4.0	4.0	----	----	5.0 Max.
Inconel 550	0.04	15.0	Bal.	----	---	---	1.0	2.50	1.15	6.70

The alloys were obtained from the manufacturer as 5/8-inch-diameter wrought bar stock. This was cut into $5\frac{1}{2}$-inch lengths which were then heat-treated as follows:

(1) S-816: Solution treated 1 hour at 2150° F and water quenched; aged 16 hours at 1400° F and air cooled.

(2) Inconel 550: Solution treated 1 hour at 2150° F and air cooled; aged 4 hours at 1600° F and air cooled; aged 4 hours at 1350° F and air cooled.

The microstructures of the two alloys after heat treatment are shown in figures 6(a) and (b). Both alloys have an austenitic (face-centered cubic) matrix structure in which precipitates have formed - carbides in S-816 and an $Ni_3(Ti,Al)$ intermetallic compound in Inconel 550.

The alloys in the heat-treated condition had a Vickers hardness number (VHN) of 269 for S-816 and 327 for Inconel 550. The specimens were machined from the heat-treated lengths of bar stock.

Procedure

The cycle through which the specimens were heated and cooled was divided into 4 parts: (1) heating to T_{max}, (2) holding at T_{max}, (3) cooling to T_{min}, and (4) holding at T_{min}.

4669

In starting a run, a specimen was held in the gripping block with
only the lower two bolts tightened. The upper two bolts were loose so
that the specimen could expand and contract freely while the initial
adjustments were being made. After the power inputs during the various
portions of the cycle had been adjusted to give the desired temperatures,
the free expansion and contraction of the test section was measured by
noting the change in scale readings when the temperature changed from
T_{max} to T_{min}. The free contractions of S-816 and Inconel 550 specimens
that were cooled from various T_{max} to a T_{min} of 200° F are plotted
in figure 7(a). Note that the two alloys contracted by nearly equal
amounts under the test conditions; the free expansion or contraction of
Inconel 550 was about 2 percent more than that of S-816.

Figure 7(b) shows the free contraction of the shoulders adjacent to
the test section during cooling from various T_{max} to a T_{min} of 200° F.

Usually about 10 cycles were required to make the adjustments and
initial readings, and the upper bolts were then tightened. In all tests
in this investigation, the upper bolts were tightened while the specimen
was at T_{max}. This induced the maximum possible tensile stress in the
specimen on cooling to T_{min}. In most of the tests T_{min} was constant
at 200° F so that the maximum tensile stress would be developed at the
same temperature, regardless of T_{max}.

The total amount of tensile deformation along the length of the
test section was measured by the difference between the change in scale
readings when the specimen was cooled while loose and while constrained.
The average strain is plotted against temperature in figure 8(a). De-
tails of the calculations are given in appendix A.

The tensile stress developed at T_{min} on the first cooling varied
with T_{max} as shown in figure 8(b). Ideally, one would expect that the
greater the temperature difference of cooling (or, in this case, the
higher the T_{max} since T_{min} was constant), the greater would be the
tensile stress at T_{min}, whereas figure 8(b) indicates a decrease in
stress at the higher ΔT values (or T_{max}). The behavior shown in fig-
ure 8(b) is due to the temperature conditions of the test method and to
the variation of the yield strength of the two alloys with temperature.

The effect of the temperature conditions follows from the manner in
which the temperature gradients changed during cooling, as shown sche-
matically in figure 9. In figure 9(a), the specimen starts cooling from
a T_{max} equal to T_1 and reaches a lower temperature T_2 shortly
thereafter; in figure 9(b), the specimen starts cooling from a T_{max}
equal to T_2. Because of the water-cooled leads attached to the shoulders

of the specimen, heat is extracted through the ends of the test section, and the ends cool more rapidly than the center of the test section. This means that, when the midpoint of the first specimen has cooled from T_1 to T_2, the other parts of its test section have cooled to lower temperatures than in the second specimen when the midpoint has just started cooling from T_2. The tensile stresses set up by the contraction of the cooler sections in the first specimen can be relieved by yielding near the midpoint, provided that this portion is still at a sufficiently high temperature for the yield strength to be low. During cooling from T_2 to T_{min}, there is less total contraction in the first specimen than in the second, and hence, the final stress at T_{min} can be less in the first specimen than in the second, depending upon the amount of yielding in the hot portion of the test section. This, in turn, depends on the temperature and the material. The tensile stress developed in Inconel 550 on cooling from a given T_{max} was always greater than that developed in S-816, due to the greater yield strength of Inconel 550.

During the first few cycles, material changes occurred that altered the electrical resistance, so that the power inputs had to be adjusted to prevent the temperatures from wandering from their proper values. The specimens soon approached an equilibrium condition, however, and there was little drift in temperatures thereafter. Strain-gage readings were taken at intervals during thermal cycling, and the average strain over the test sections varied slightly during cycling. The calculated stress changes and average strains, absorbed by the test sections after one-half of the number of cycles required for failure were run, are shown in figure 10 against the maximum cycle temperature. In figure 10(a) it is noted that the two alloys deformed almost equally up to about 1350° to 1400° F, whereas S-816 deformed more than Inconel 550 at higher temperatures. At the higher T_{max}, a significant portion of this deformation was compressive creep. This creep could be noted by the drop in scale readings as the temperature approached or was held at T_{max}, and it occurred at lower temperatures for S-816 than for Inconel 550. The stress change plotted in figure 10(b) is the difference between the tensile stress at T_{min} and the compressive stress at T_{max}. Here, as in figure 8(b) where the tensile stress developed during the first cycle of cooling, there is a drop at high values of T_{max}.

In a number of tests thermal cycling was continued until the specimens failed. Failure was defined as actual fracture across the test section, and generally occurred at/or very near the center of the test section. Immediately before failure, there was a period in which T_{max} increased because of overheating as a result of the reduction of current-carrying area that accompanied cracking. This overheating period lasted for five to ten cycles at high T_{max} and increased in duration as the T_{max} was lowered so that it was on the order of several percent of the

total number of cycles to failure. No further heating could occur after
failure, and the number of cycles to failure was easily determined from
the charts of temperature against time.

The diameters of the specimens were measured with micrometers both
before and after removal from thermal cycling. Most of the specimens
were bulged at the center of the test section because of compressive
yielding and creep at T_{max}. The amount of bulging increased as T_{max}
increased, as shown in figure 11, and was offset by a slight thinning to
either side of the bulge.

Microstructures and hardnesses were also studied. Specimens for
these metallographic studies were prepared by carefully machining flat
surfaces through the central planes. Hardness was measured with a micro-
hardness tester, using a Vickers diamond penetrator and a 1-kilogram
load, and the measurements were made 0.01 inch below the fracture edge.

<div align="center">RESULTS AND DISCUSSION</div>

The results from specimens that were cycled to failure under varying
conditions of thermal fatigue indicated the following effects of the cycle
variables on the number of cycles to failure.

<div align="center">Effect of Maximum Cycle Temperature and Temperature</div>

<div align="center">Difference of Cycling</div>

For the conditions of testing, N_f was governed more strongly by
T_{max} than by ΔT. This is shown in figure 12. The solid curves at a
constant ΔT of 1150° F in figure 12 show the variation in N_f with
T_{max}, and the dashed curves at a constant T_{min} of 200° F show the vari-
ation in N_f under the combined effects of T_{max} and ΔT. If ΔT were
the sole factor controlling N_f, the solid curves would be straight,
vertical lines intersecting the dashed curves at a common point
($T_{max} = 1350°$ F, $T_{min} = 200°$ F, $\Delta T = 1150°$ F)[2]; in other words, N_f would

_____

[2]This common point of intersection can be observed in the results
for Inconel 550 plotted in figure 12(a). In the case of S-816, however,
the specimens for the two curves were taken from different bars of mate-
rial, and the one bar was stronger than the other. Hence, the two curves
for S-816 in figure 12(b) are offset from one another. However, despite
this offset, the two curves for S-816 show the same relative behavior of
decreasing N_f with increasing T_{max} as the curves for Inconel 550.
In all subsequent tests where comparisons were made, care was taken to
eliminate bar-to-bar variations in material by using specimens from the
same bar or from bars that were shown to be equivalent.

be constant as long as ΔT was constant. The actual curves at constant ΔT are not vertical, and the amount by which the actual curves deviate from the vertical indicates the effect of different T_{max}. For both alloys, the decrease in N_f due to increasing T_{max} at a constant ΔT was almost as severe as the decrease in N_f due to increasing both T_{max} and ΔT simultaneously.

Additional tests on Inconel 550 confirmed the strong effect of T_{max} on N_f. Results of these tests are plotted in the solid curve in figure 13, which shows the variation in N_f with ΔT at a constant T_{max} of 1550° F. The dashed curve of figure 13 that is plotted for comparison shows the variation in N_f with ΔT at a constant T_{min} of 200° F. (The dashed curve is the same as that in fig. 12(a); it has been replotted in figure 13 against the ordinate ΔT rather than T_{max}. Note that the point of intersection of the two curves in fig. 13 is a common point, $T_{max} = 1550^{\circ}$ F, $T_{min} = 200^{\circ}$ F, $\Delta T = 1350^{\circ}$ F.) If T_{max} were completely controlling, the solid curve in figure 13 would be a straight, vertical line. Actually, it is not vertical, and this shows that ΔT also has an effect on N_f. However, as the two curves indicate, increasing or decreasing ΔT and T_{max} simultaneously (dashed curve) had much more effect on N_f than increasing or decreasing ΔT without changing T_{max} (solid curve).

The results can be presented in other ways that indicate numerically the relative importance of T_{max} and ΔT for a limited range of conditions. For example, as indicated in the following diagram, Inconel 550 endured about 860 cycles before failing when cycled between 1550° and 400° F. If ΔT was reduced 200° F by raising T_{min} to 600° F while maintaining T_{max} at 1550° F, the life was increased to 1700 cycles; that is, reducing ΔT by 200° F for constant T_{max} approximately doubled N_f. On the other hand, if T_{max} was reduced 200° to 1350° F while maintaining ΔT at 1150° F, the life was increased to 10,500 cycles. Thus, under these conditions, the increase in N_f due to reducing T_{max} by 200° F was more than 11 times the increase obtained by reducing ΔT by the same amount.

$$1550^{\circ}/400^{\circ} \text{ F}$$
$$N_f = 860 \text{ cycles}$$

Reduce ΔT by 200° F   Reduce T_{max} by 200° F
  at constant T_{max} at constant ΔT

$1550^{\circ}/600^{\circ}$ F $1350^{\circ}/200^{\circ}$ F
$N_f = 1700$ cycles $N_f = 10,500$ cycles
$$\underline{1700}$$ $$\underline{10,500}$$
-860 -860
Improvement = 840 cycles   Improvement = 9,640 cycles
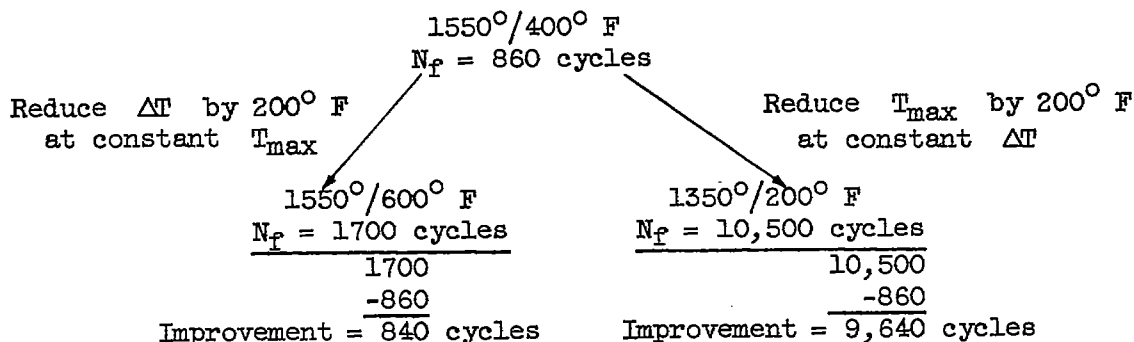
The numerical value calculated from this diagram for the relative importance of T_{max} and ΔT is correct only for a particular set of conditions. Other conditions can increase or decrease this relative importance. The concentration of deformation in the center of the test section, due to the manner of heating and cooling, as discussed earlier, has probably emphasized the effect of T_{max} in the experimental results. Under less severe conditions, ΔT could be more important than has been found here. Obviously, no fracture would occur unless there was a ΔT, regardless of how near T_{max} might approach the melting point of the material, since without a ΔT there would be no strain change.

The point emphasized by the results is that T_{max} is an important factor in thermal fatigue, and the life in thermal fatigue is not determined by ΔT alone. The effect of T_{max} superimposed on that of ΔT can overshadow the effect of ΔT alone. In view of its importance on life, the effect of T_{max} can hardly be overemphasized in an analysis of thermal fatigue.

Although increasing T_{max} reduced the thermal-fatigue life, the reduction was not always as great as one might expect by simply extrapolating the results at lower T_{max}. Thus, as the results for S-816 plotted in figure 12(b) indicate, the decrease in life with increasing T_{max} for a constant T_{min} of 200° F was approximately linear on a semilog plot at low values of T_{max}, and the curve then swung upwards at T_{max} above about 1450° F. This upward swing was not obtained in the data for Inconel 550 over the same temperature range. As a result, the curves for the two alloys crossed one another in the manner shown in figure 14. As figure 14 shows, Inconel 550 had a better thermal-fatigue life than S-816 at T_{max} below 1525° F, whereas S-816 endured more cycles to failure at higher T_{max}.

This variation of the thermal-fatigue life with T_{max} appears related to the effect of T_{max} on the hardness behavior of the two alloys. Figure 15 is a plot of the change in hardness of the specimens cycled between different T_{max} and a constant T_{min} of 200° F. The hardness change is the increase in hardness measured on the fractured specimens as compared with their initial hardness before thermal fatigue (i.e., the hardness in the as-heat-treated condition). The final hardness readings were taken just below the fracture edges. As figure 15 shows, S-816 underwent considerable hardening during exposure to thermal-fatigue conditions, either as a result of strain-hardening, or additional precipitation-hardening, or both. The maximum hardening occurred at a T_{max} of 1450° F, and at higher T_{max} there was a softening relative to this maximum. Inconel 550, on the other hand, was initially harder than S-816 and did not change hardness during cycling; at most, there was a slight softening

at T_{max} above 1500° F. Comparison of the effects of T_{max} on the life
(fig. 14) and the hardening (fig. 15) shows that the upward swing in the
life of S-816 occurs at the temperature of maximum hardening, whereas no
upward swing occurs in the life curve of Inconel 550. It appears, then,
that softening at high temperatures restored the ductility of S-816 so
that it could absorb more cycles of thermal fatigue than it could have
otherwise. Thus, the protection due to relative softening gave S-816 a
longer life than Inconel 550 at high T_{max}, whereas at low T_{max} Inconel
550 endured more cycles to failure.

Photomicrographs of S-816 specimens that had failed in thermal-
fatigue tests are shown in figures 16(a), (b), and (c). Note that the
fracture in all cases was transcrystalline. All specimens showed addi-
tional precipitation during thermal fatigue. For the specimen cycled at
a T_{max} of 1450° F (fig. 16(b)), the additional precipitation is well
defined and is seen to occur principally along slip planes. Additional
precipitation was somewhat less at a T_{max} of 1200° F, but was still
evident along some slip planes (fig. 16(a)). At a T_{max} of 1600° F, the
slip planes are again marked by additional precipitation, but instead of
being straight, the slip planes are curved and distorted (fig. 16(c)).
In addition, many of the particles of precipitate have spheroidized at
the high T_{max}. These changes were consistent with the hardness behavior.

Photomicrographs of Inconel 550 specimens that had failed in thermal
fatigue are shown in figures 16(d) to (h). As in the case of S-816,
all failures were transcrystalline. There was no marked increase in
precipitation in these specimens. Note the manner in which the grain
boundaries have broken into steps in the specimens cycled at T_{max} of
1350° and 1550° F (figs. 16(d) and (e)), and also to the twinning in the
lower grain in figure 16(d). At a T_{max} of 1600° F, recrystallization
along slip planes was especially pronounced (figs. 16(f) and (g), and
especially, fig. 16(h)), although it could be observed at T_{max} as low as
1450° F. Also, the formation of voids was very evident at the T_{max} of
1600° F (e.g., fig. 16(f)).

Effect of Time at Maximum Cycle Temperature

The time of exposure at T_{max} also affected N_f as shown in fig-
ure 17. This effect was studied by increasing the hold time at T_{max}
from 15 seconds to 1 minute. For both alloys, increasing the hold time
at T_{max} by a factor of four increased N_f at high T_{max} and decreased
N_f at low T_{max}. The crossover points were at 1360° F for S-816 and at
1510° F for Inconel 550, and the effect of time appeared more pronounced
for S-816 than for Inconel 550.

Although the effect of the time at T_{max} appears small, particularly for Inconel 550, it is significant that it can be observed in relatively short times. Where parts in service are maintained at high temperatures for much longer times than the experimental cycles used here, the effect may be more severe. The disagreement between short-time thermal-shock tests in the laboratory and service lives may be partially due to this effect of time.

Photomicrographs of specimens of S-816 and Inconel 550 that had been fractured at temperatures below the crossover points are shown in figure 18. Additional precipitation was very evident in both alloys. Note the twinning, grain boundary fragmentation, and "steps" produced within the grains of the Inconel 550 specimen.

Effect of Strain Change

Attempts to correlate the number of cycles to failure with the amount of plastic deformation per half cycle by the equation

$$N_f = K\epsilon_p^{-n} \tag{1}$$

were unsuccessful, as indicated by the data for S-816 plotted in figure 19. For equation (1) to be valid, the log-log method of plotting in figure 19 should reduce the data to a single straight line, which is obviously not the case. Although the results for a single series of tests, such as those at constant T_{min} (circles, fig. 19), might be satisfied by a straight line for a limited range or for low values of T_{max}, the curve sweeps upwards at high T_{max} so that N_f is greater than would be predicted by a straight-line extrapolation of the results at low T_{max}. Results for a series of tests at constant ΔT (diamonds, fig. 19)[3] are considerably different from the results at constant T_{min}. Although there was very little variation in the average plastic strain per half cycle for the three specimens at constant ΔT, N_f was significantly reduced as T_{max} increased.

It must be admitted that the calculation of the plastic strain per half cycle, both in the present tests and in those of Coffin (refs. 16 to 19), involves some errors and approximations. Details are given in appendix B. The most serious error is the fact that the strain was not uniform along the test section due to the temperature gradient and the manner of heating and cooling, as discussed earlier. Ideally, the plastic strain should be evaluated in the narrow section at the center of the test

---

[3]The three specimens tested at constant ΔT were from a different bar of material than those tested at constant T_{min}, so that the point for $T_{max} = 1350°$ F, $T_{min} = 200°$ F is not common (discussed in footnote 2).

section where fracture occurred. Actually, the higher the T_{max}, the more the calculated average plastic strain (ordinate in fig. 19) was concentrated in the area of the fracture. It appears doubtful, however, that correcting the average plastic strain over the test section to the actual plastic strain in the region of fracture would reduce all of the data points plotted in figure 19 to a single straight line. The test conditions, particularly T_{max}, appear to be important factors in addition to the cyclic strain. For example, when the cyclic time of exposure was increased at high values of T_{max}, the cyclic plastic strain was also increased by virtue of the creep strain that occurred during the longer time of holding; nevertheless, despite this increase in strain, the number of cycles to failure was increased by the increase in holding time, rather than reduced, as would be required by equation (1). Thus, it is concluded that the number of cycles to failure is not governed solely by the cyclic plastic strain and that equation (1) must be modified by additional terms defining the test conditions in order to have general applicability.

<div align="center">CONCLUSIONS</div>

The following conclusions have been drawn from a study of the effect of the test conditions on the number of cycles to failure in thermal fatigue for the materials and test conditions studied:

1. The number of cycles to failure was more sensitive to changes in the maximum cycle temperature than to changes in the temperature difference.

2. Increasing the time of exposure at high maximum cycle temperatures increased the number of cycles to failure, whereas the same increase in time at low maximum cycle temperatures decreased the number of cycles to failure.

3. The number of cycles to failure depends upon temperature and time effects in addition to the thermal strains absorbed by plastic flow in the materials.

Lewis Flight Propulsion Laboratory
    National Advisory Committee for Aeronautics
        Cleveland, Ohio, June 30, 1958

APPENDIX A

CALCULATION OF STRESS AND AVERAGE TOTAL STRAIN IN TEST SECTION DURING

CONSTRAINED COOLING FROM MAXIMUM TO MINIMUM CYCLE TEMPERATURE

The nomenclature used in this appendix is as follows:

A = scale movement of strain gage on test section of specimen during
     cooling from T_{max} to T_{min} while loose, in.

B = scale movement of strain gage on test section of specimen during
     cooling from T_{max} to T_{min} while constrained, in.

C = magnification factor of strain gage

D = scale movement of dial gage at loose end of specimen during cooling
     from T_{max} to T_{min} while loose, in.

E = modulus of elasticity of material, psi

    In addition to the above symbols, the letters X and X' are used
in the following derivation to refer to the positions of the opposite
ends of the specimen, as indicated in figure 1, the letters Y and Y'
refer to the positions of the outer ends of the shoulders adjacent to the
test section, and the letters Z and Z' refer to the positions of the
opposite ends of the test section.

    When the specimen is cooled from T_{max} to T_{min} while loose,
points Z and Z' move together the amount A/C, and points X and X'
move together the amount D. Since the large shoulders at opposite ends
undergo no temperature change during heating and cooling the test section,
the points Y and Y' also move together an amount D. Thus, the free
contraction of the test section is A/C and that of the two adjacent
shoulders is D - A/C.

    When the same cooling is repeated while the specimen is constrained,
the points Z and Z' move together an amount B/C (where B/C < A/C),
and points Y and Y' (as well as X and X') do not move since they
are held fixed by the gripping block. In this case, the test section
must therefore be stretched the amount A/C - B/C = (A - B)/C. At the
same time, the adjacent shoulders are pulled out the amount D - A/C
that they would have contracted because of free cooling plus the addi-
tional amount B/C; that is, the adjacent shoulders have been stretched
the amount D - A/C + B/C = D - (A - B)/C.

The amount of elastic and plastic deformation that the test section undergoes during constrained cooling in order to absorb the thermal strain is therefore equal to $(A - B)/C$. Dividing this quantity by the length of the test section, which is $1/2$ inch, gives the average total strain, which is plotted in figure 8(a) for the first cycle of constrained cooling and in figure 10(a) at $N = \frac{1}{2}N_f$.

In order to calculate the stress in the test section, the stress in the shoulders was first calculated by multiplying the strain in the shoulders by the modulus of elasticity. Since the length of the shoulders adjacent to the test section was 2 inches, this gives

$$\left(D - \frac{A - B}{C}\right) \times \frac{1}{2} \times E$$

for the stress in the shoulders. Multiplying this quantity by the ratio of the cross-sectional areas of the shoulders and the test section gives the stress in the test section, which is plotted in figures 8(b) and 10(b).

4669

CE-4

APPENDIX B

CALCULATION OF AVERAGE PLASTIC STRAIN IN TEST SECTION DURING

CONSTRAINED COOLING FROM MAXIMUM TO MINIMUM CYCLIC TEMPERATURE

The average total strain in the test section and the stress in the test section were calculated by the method described in appendix A. This was done for the cycle $N = 1/2 \, N_f$. The elastic strain in the test section was next calculated by dividing the stress by the modulus of elasticity. The modulus of elasticity was evaluated at the average temperature of T_{max} and T_{min}. The average plastic strain was then calculated by subtracting the elastic strain from the total strain, and this is the quantity plotted in figure 19.

REFERENCES

1. Stewart, W. C., and Schreitz, W. G.: Thermal-Shock and Other Comparison Tests of Austenitic and Ferritic Steels for Main Steam Piping. Trans. ASME, vol. 72, no. 7, Oct. 1950, pp. 1043-1055; discussion, pp. 1055-1060.

2. Stewart, W. C., and Schreitz, W. G.: Thermal-Shock and Other Comparison Tests of Austenitic and Ferritic Steels for Main Steam Piping - A Summary Report. Trans. ASME, vol. 75, no. 6, Aug. 1953, pp. 1051-1068; discussion, pp. 1068-1072.

3. Dixon, E. S.: Needs of the Oil Industry for Metals at High Temperatures. Symposium on Effect of Temperature on the Properties of Metals, publ. by ASTM-ASME, June 23, 1932, pp. 68-84.

4. Holmberg, M. E.: Experience with Austenitic Steels in High-Temperature Service in the Petroleum Industry. Trans. ASME, vol. 73, no. 6, Aug. 1951, pp. 733-739; discussion, pp. 739-742.

5. Rutherford, John J. V.: Some Experience in Service (Power, Oil and Chemical Plants). High Temperature Properties of Metals, ASM, 1951, pp. 133-170.

6. Weeton, John W.: Mechanisms of Failure of High Nickel-Alloy Turbojet Combustion Liners. NACA TN 1938, 1949.

7. Garrett, Floyd B., and Yaker, Charles: Turbojet-Engine Evaluation of AISI 321 and AISI 347 Stainless Steel as Nozzle-Blade Materials. NACA RM E9K17, 1950.

8. Millenson, M. B., and Manson, S. S.: Investigation of Rim Cracking
     in Turbine Wheels with Welded Blades. NACA RN E6L17, 1947.

9. Wilterdink, P. I.: Experimental Investigation of Rim Cracking in
     Disks Subjected to High Temperature Gradients. NACA RM E9F16, 1949.

10. Wilterdink, P. I., Holms, A. G., and Manson, S. S.: A Theoretical
      and Experimental Investigation of the Influence of Temperature
      Gradients on the Deformation and Burst Speeds of Rotating Disks.
      NACA TN 2803, 1952.

11. Thompson, A. S.: Thermal Stress in Power-Producing Elements. Jour.
      Aero. Sci., vol. 19, no. 7, July 1952, pp. 476-480.

12. Clauss, Francis J., and Freeman, James W.: Thermal Fatigue of Ductile
      Materials. II - Effect of Cyclic Thermal Stressing on the Stress-
      Rupture Life and Ductility of S-816 and Inconel 550. NACA TN 4165,
      1958.

13. Bentele, M., and Lowthian, C. S.: Thermal Shock Tests on Gas Turbine
      Materials. Aircraft Eng., vol. XXIV, no. 276, Feb. 1952, pp. 32-38.

14. Whitman, M. J., Hall, R. W., and Yaker, C.: Resistance of Six Cast
      High-Temperature Alloys to Cracking Caused by Thermal Shock. NACA
      TN 2037, 1950.

15. Anon.: Thermal Shock Properties of High Temperature Alloys. Res.
      Labs., Allegheny Ludlum Steel Corp. (N.Y.), Nov. 24, 1954.

16. Coffin, L. F., Jr., and Wesley, R. P.: Apparatus for the Study of
      Effects of Cyclic Thermal Stresses on Ductile Materials. Trans.
      ASME, vol. 76, Aug. 1954, pp. 923-930.

17. Coffin, L. F., Jr.: A Study of the Effects of Cyclic Thermal Stresses
      on a Ductile Material. Trans. ASME, vol. 76, Aug. 1954, pp. 931-
      949; discussion, pp. 949-950.

18. Coffin, L. F., Jr.: The Problem of Thermal Stress Fatigue on Austen-
      itic Steels at Elevated Temperature. Symposium on Effect of Cyclic
      Heating and Stressing on Metals at Elevated Temperatures, Spec.
      Tech. Pub. 169, ASTM, 1954, pp. 31-50; discussion, pp. 51-52.

19. Coffin, L. F., Jr.: Design Aspects of High Temperature Fatigue with
      Particular Reference to Thermal Stresses. Trans. ASME, vol. 78,
      no. 3, Apr. 1956, pp. 527-532.

20. Manson, S. S.: Behavior of Materials Under Conditions of Thermal
      Stress. NACA Rep. 1170, 1954. (Supersedes NACA TN 2933.)

21. Liu, S. I., Lynch, J. J., Ripling, E. J., and Sachs, G.: Low Cycle Fatigue of the Aluminum Alloy 24S-T in Direct Stress. Trans. AIME, vol. 175, 1948, pp. 469-496.

4669

CB-4 back
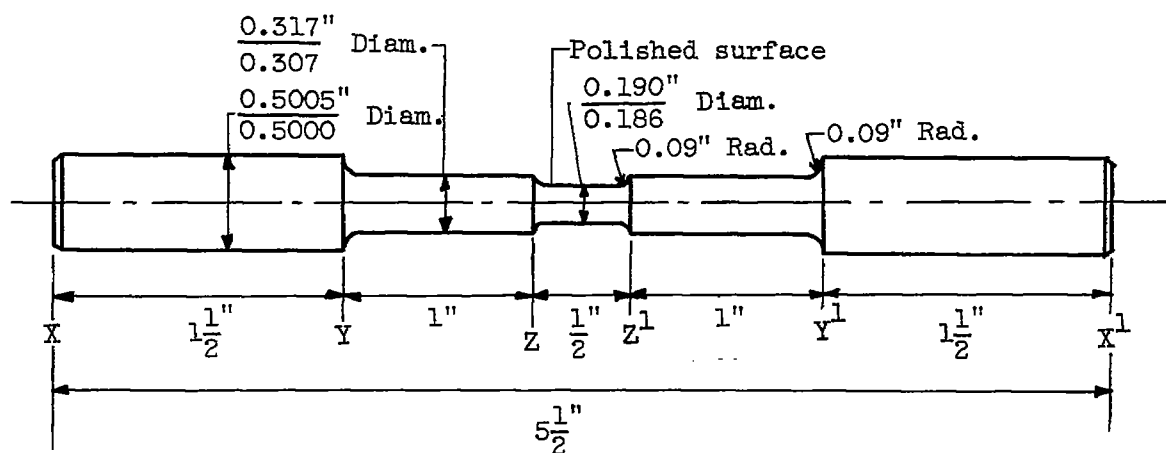
Figure 1. - Test specimen.
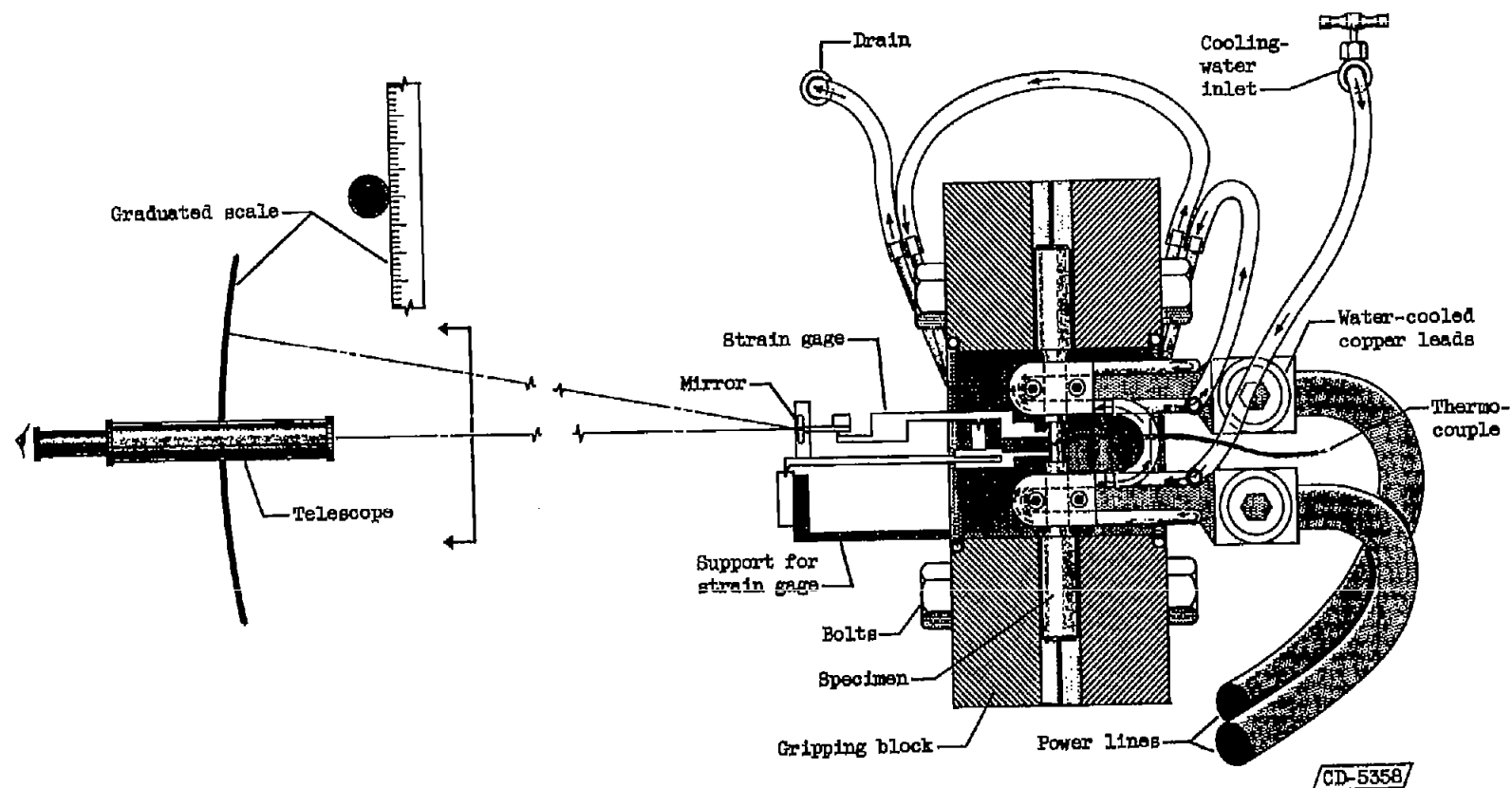
Figure 2. - Diagram of equipment.
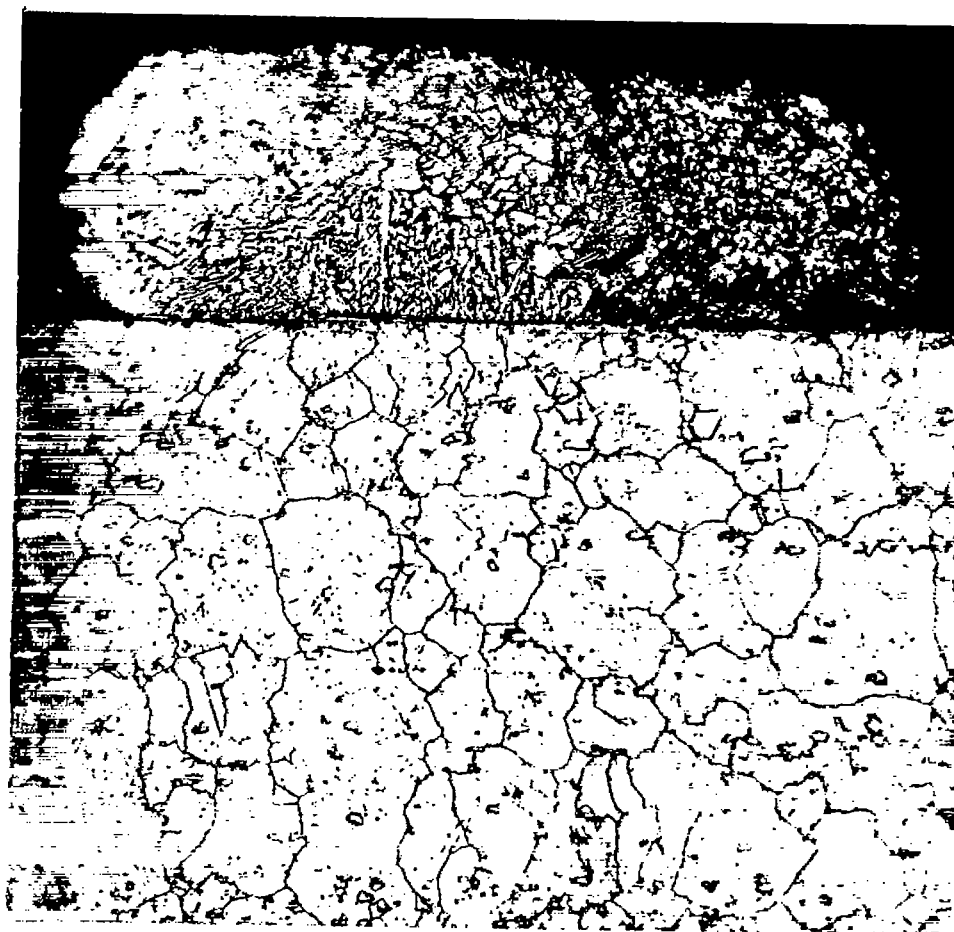
C-48023

Figure 3. - Thermocouple wires spot-welded to S-816 specimen
(specimen had been cycled 200 times between 1350° and 200° F).
Electrolytically etched in a dilute solution of nitric and
hydrochloric acids. X250.
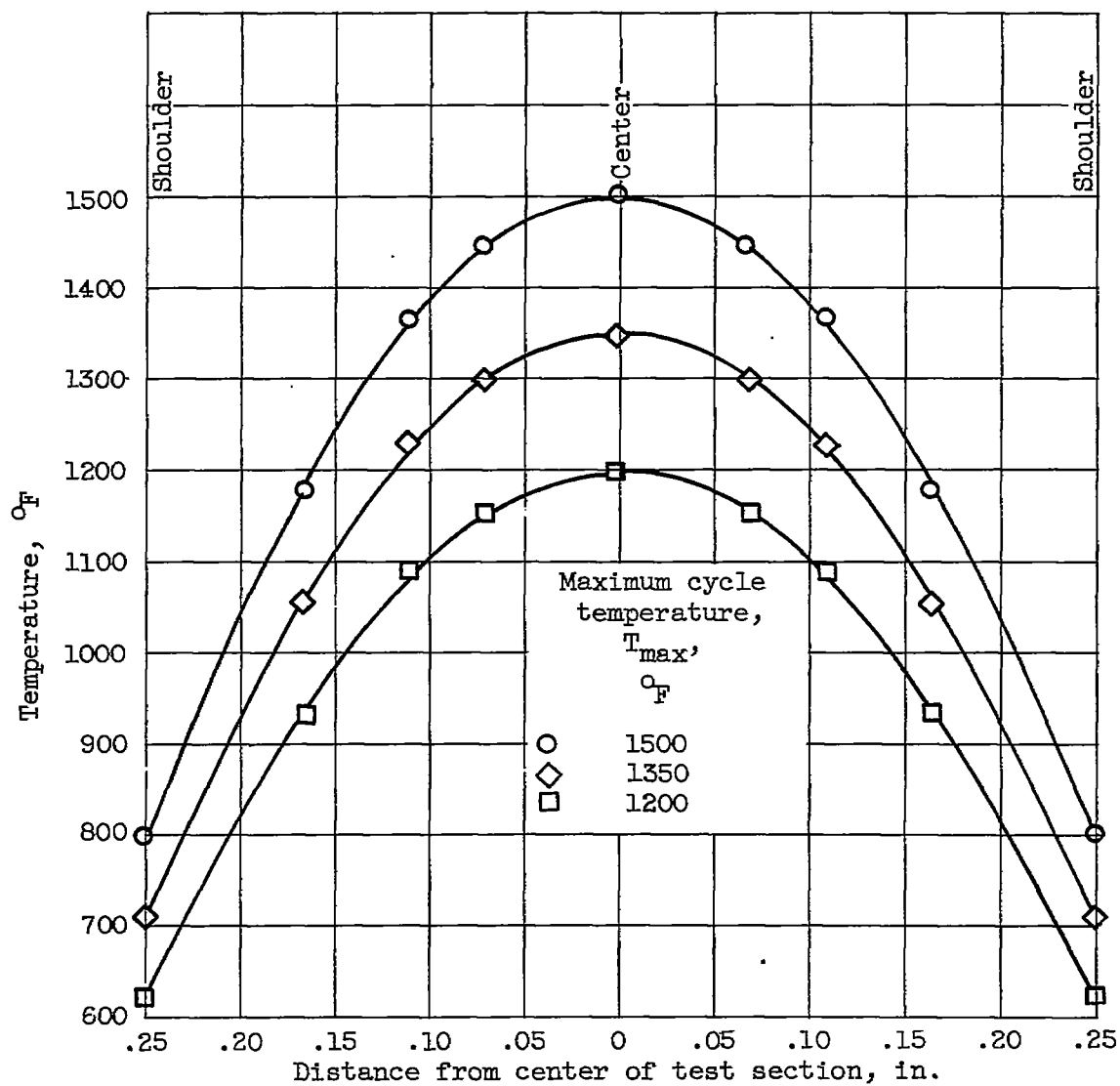
Figure 4. - Temperature profiles of test specimens.
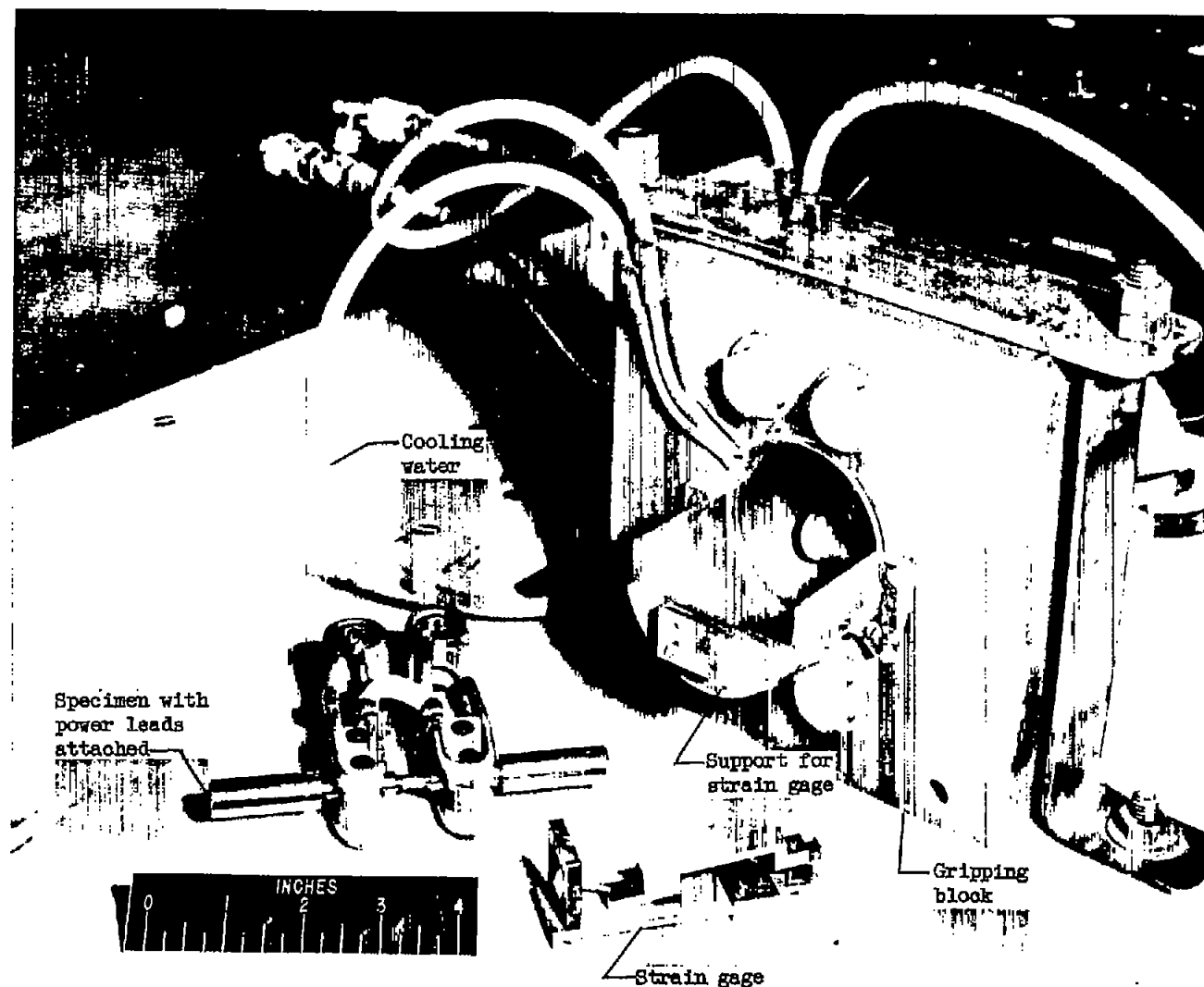
Figure 5. - Photograph of equipment.

C-40734
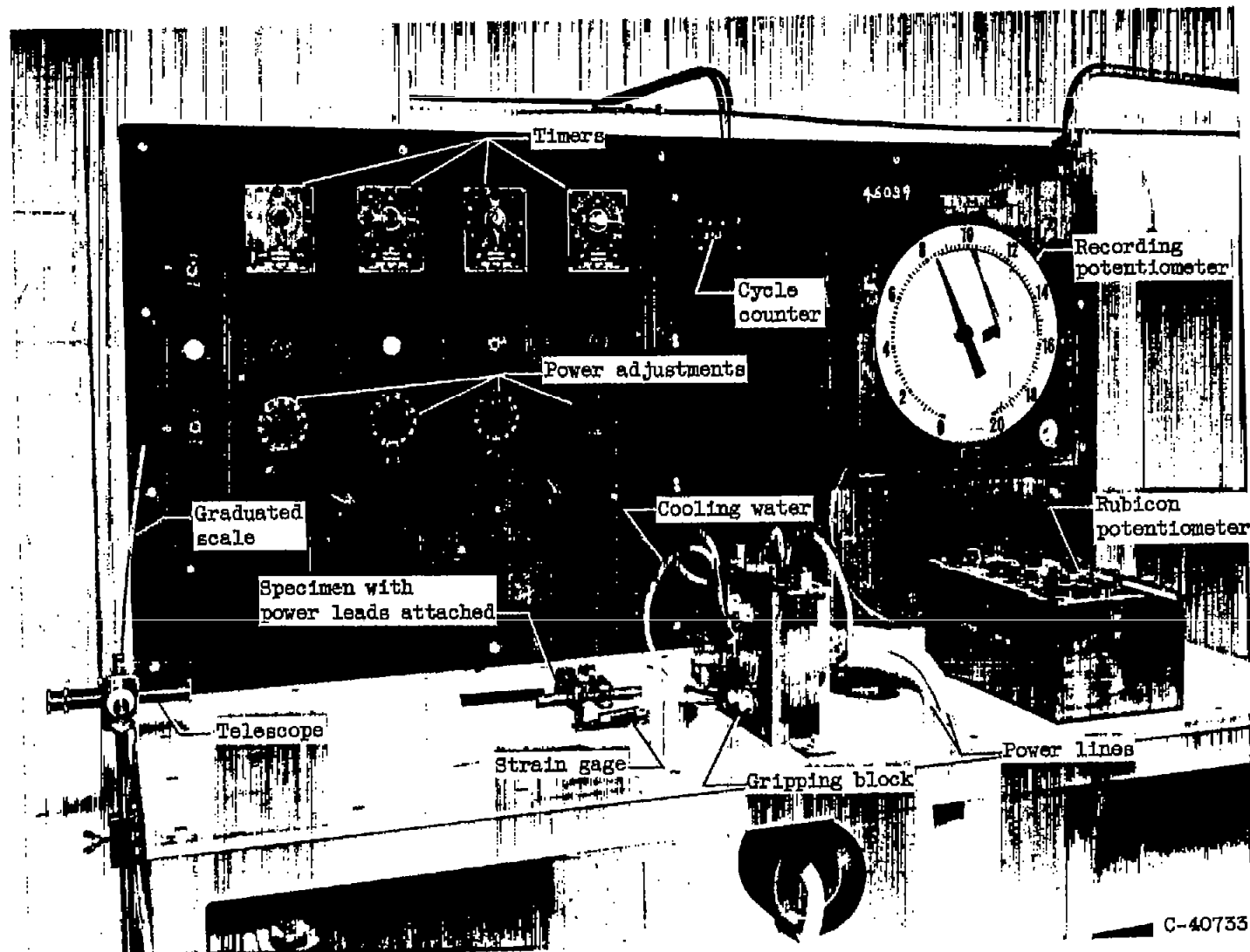
Figure 5. - Concluded. Photograph of equipment.
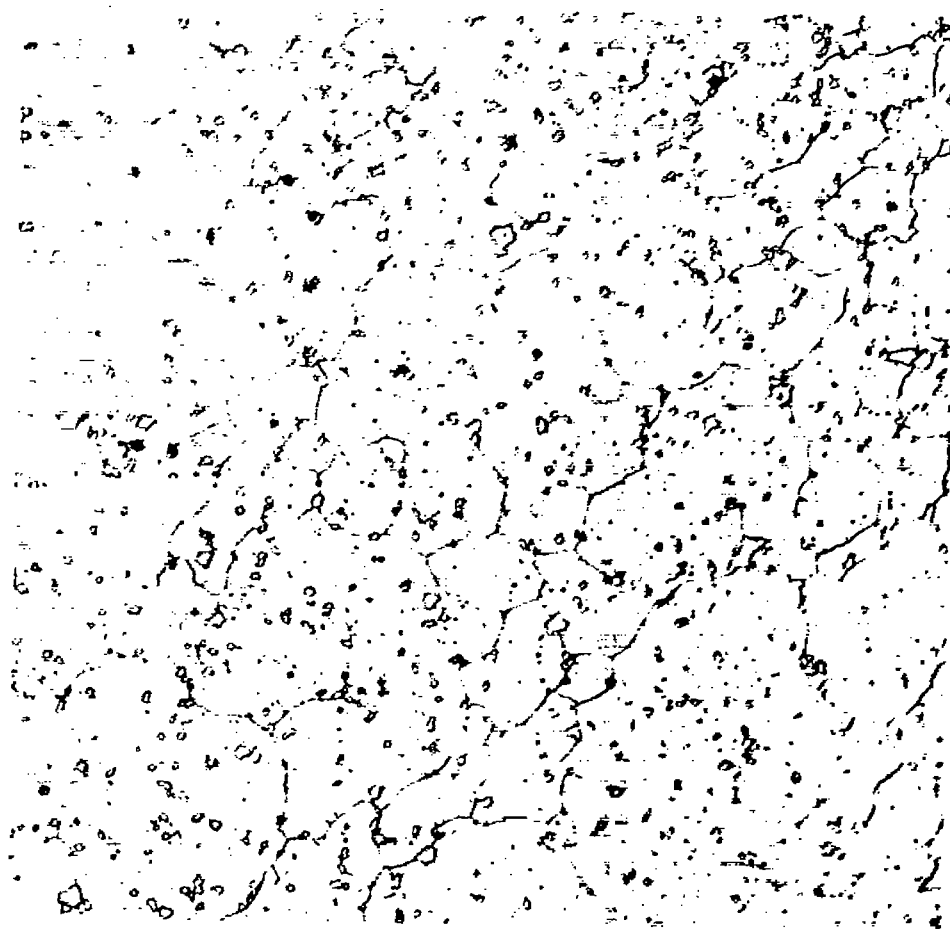
C-48024

(a) S-816 electrolytically etched in a dilute solution of sulfuric and boric acids.

Figure 6. - Microstructure of heat-treated specimen before test. X250.
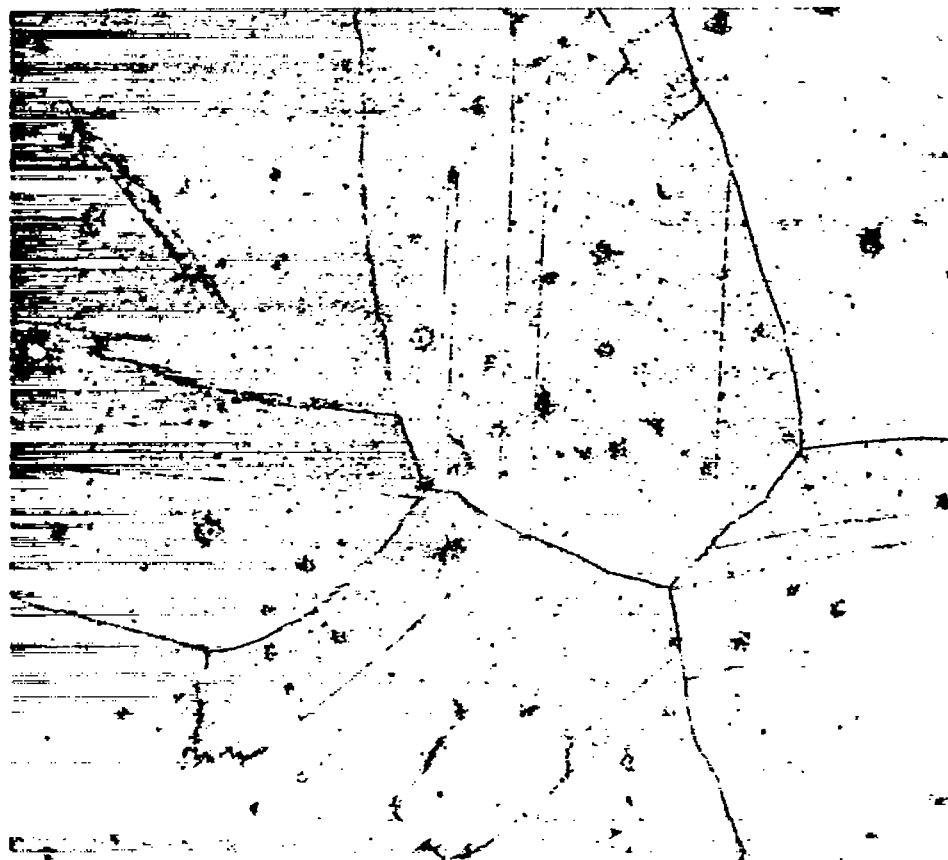
C-48025

(b) Inconel 550 electrolytically etched in a dilute solution of
    hydrofluoric acid and glycerol in water.

Figure 6. - Concluded. Microstructure of heat-treated specimen
    before test. X250.
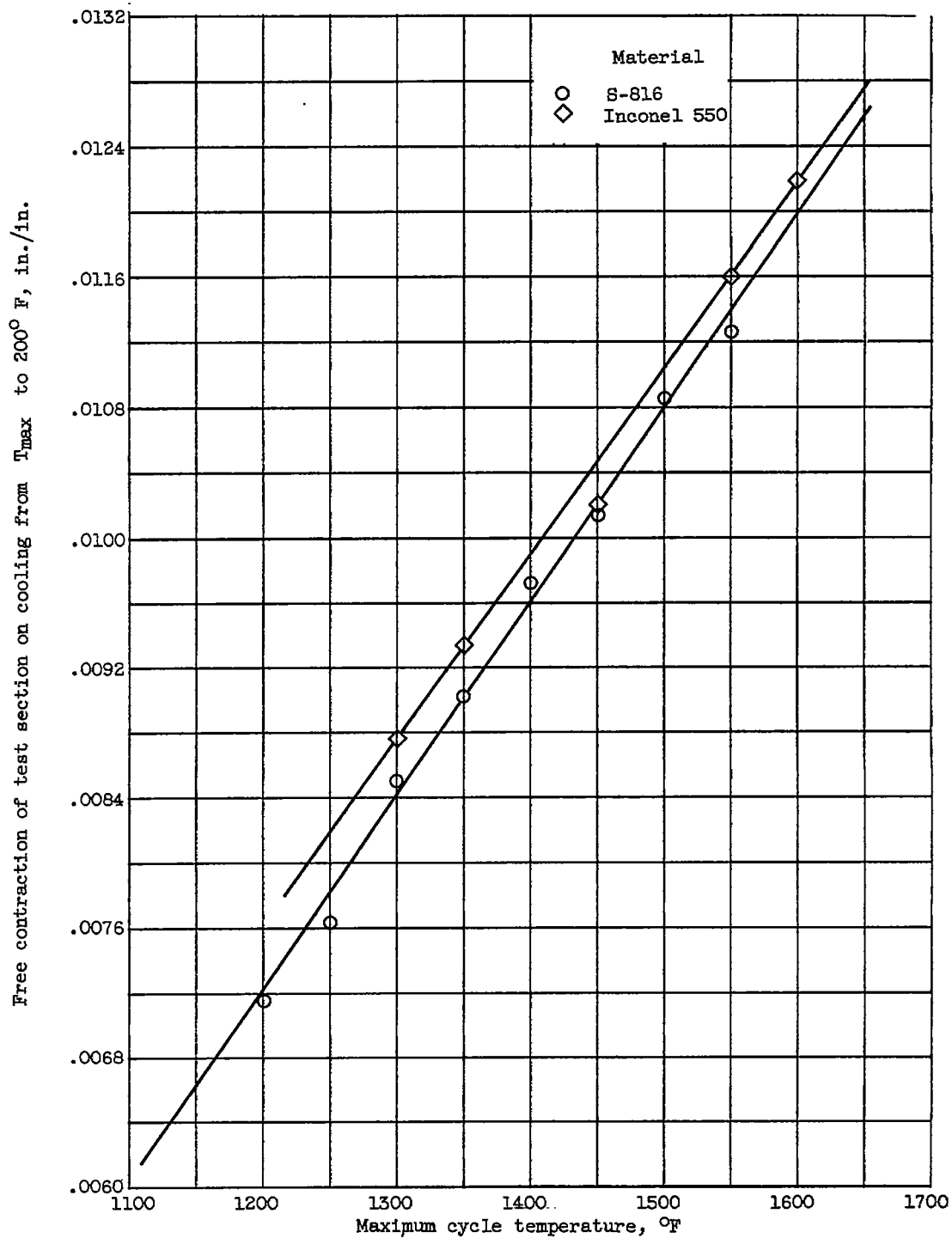
(a) Contraction of test section.

Figure 7. - Free contraction of S-816 and Inconel 550 during cooling from
various maximum temperatures to a minimum temperature of 200° F.
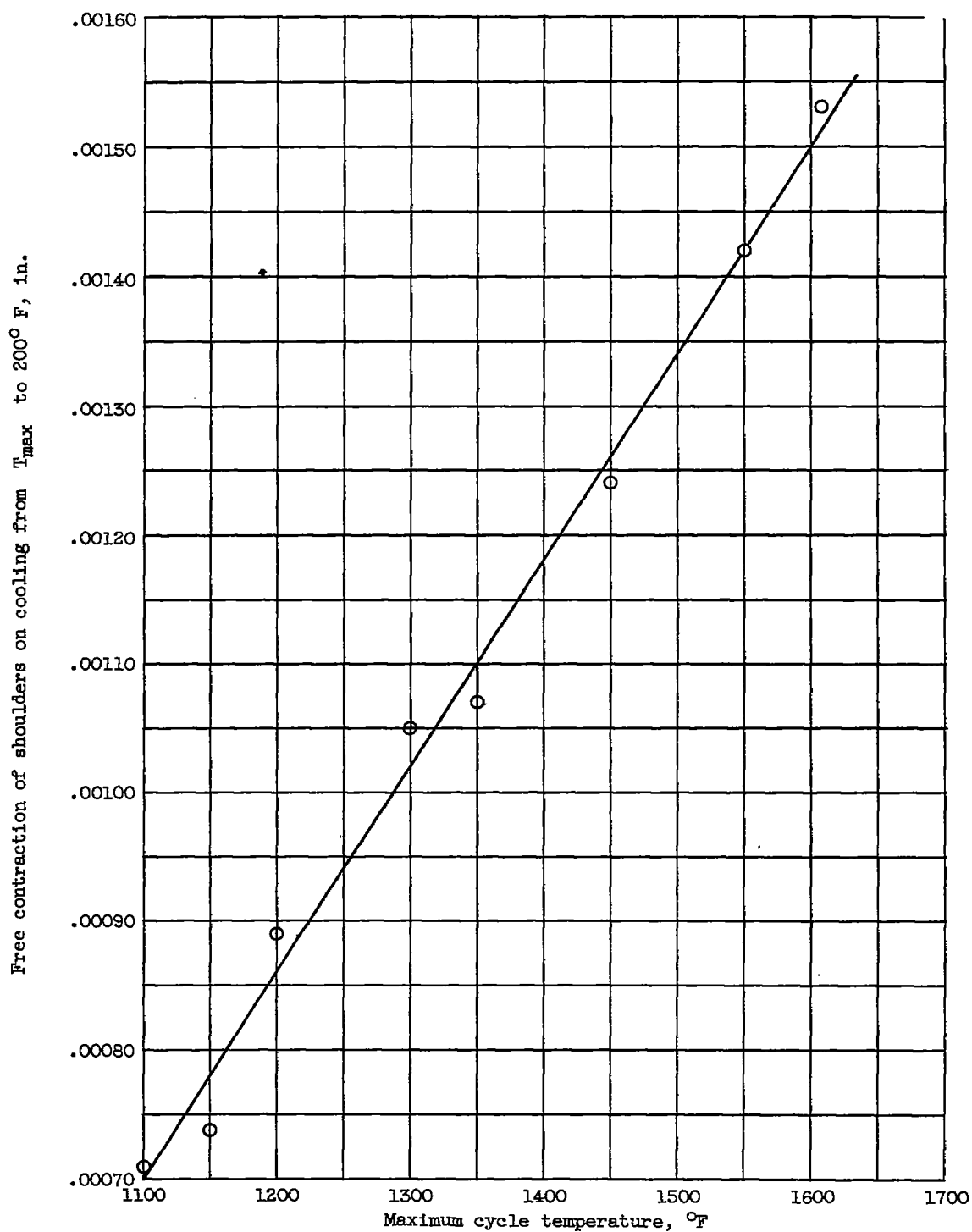
(b) Contraction of shoulder adjacent to test section.

Figure 7. - Concluded. Free contraction of S-816 and Inconel 550 during
cooling from various maximum temperatures to a minimum temperature of
200° F.
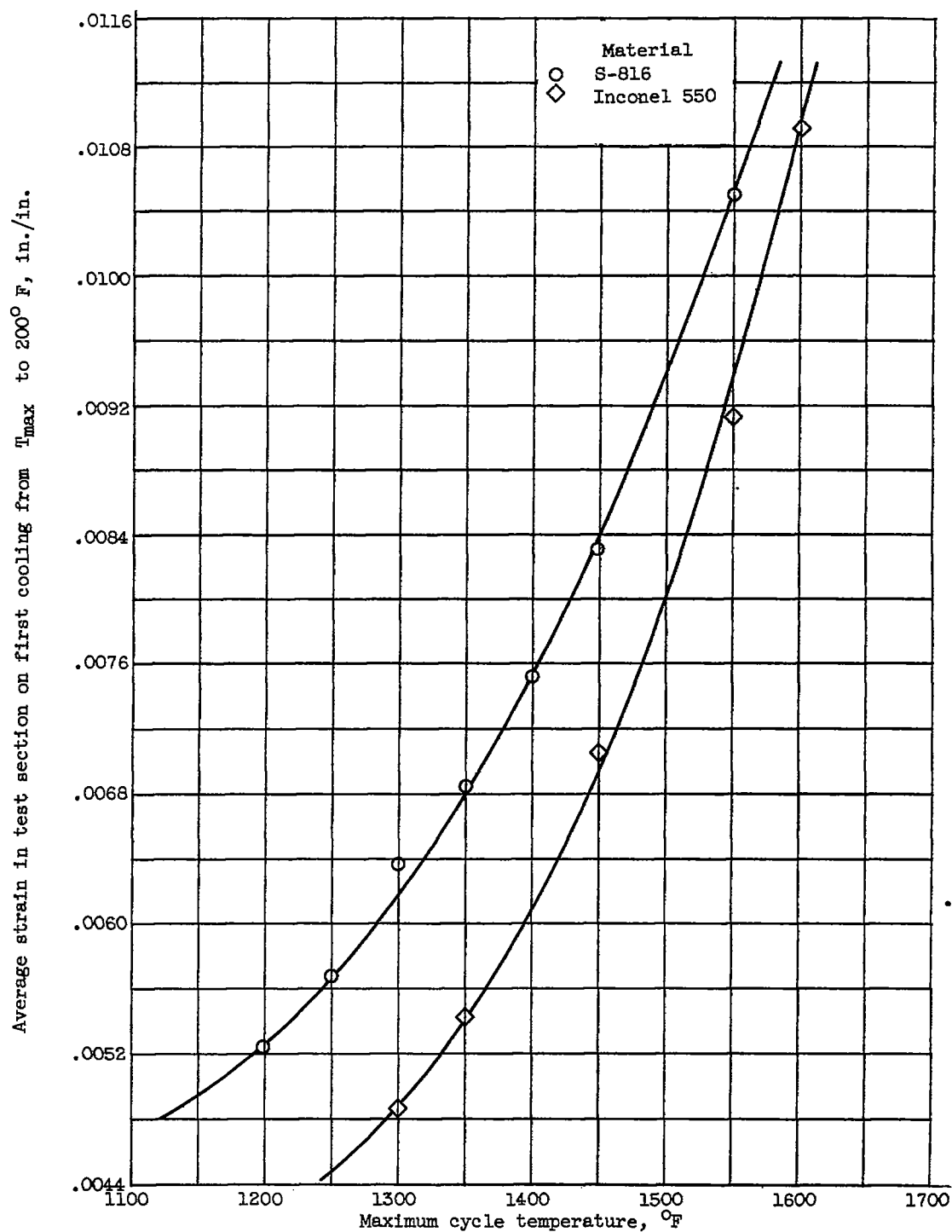
(a) Average strain.

Figure 8. - Stress and strain in test section during first cycle of con-
strained cooling from various maximum temperatures to a minimum tempera-
ture of 200° F.
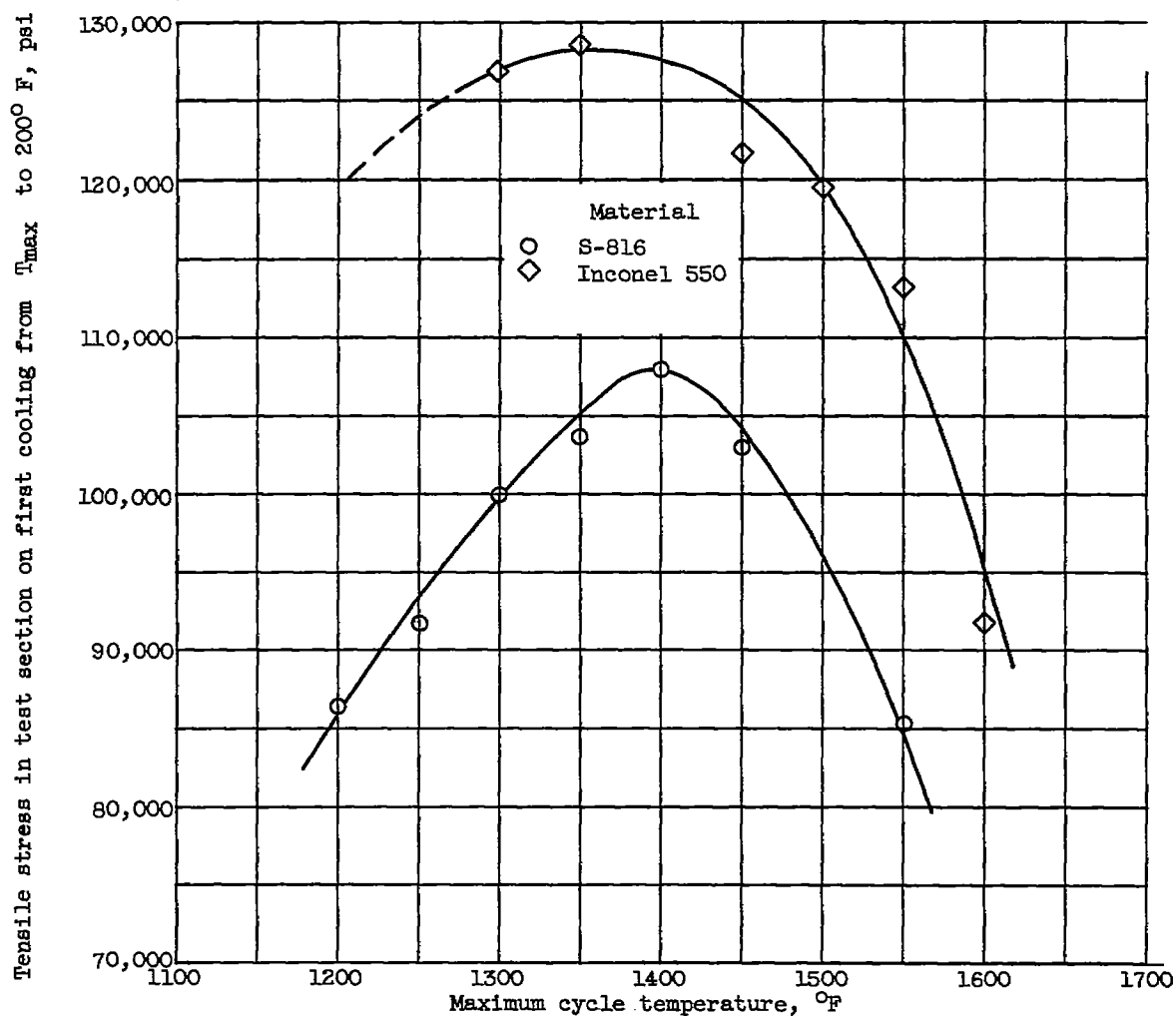
(b) Tensile stress.

Figure 8. - Concluded. Stress and strain in test section during first cycle
   of constrained cooling from various maximum temperatures to a minimum tem-
   perature of 200° F.
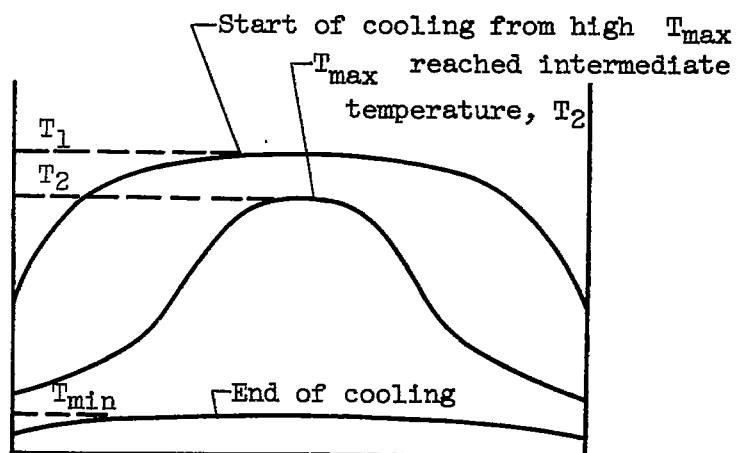
Temperature

(a) Cooling from $T_{max} = T_1$.
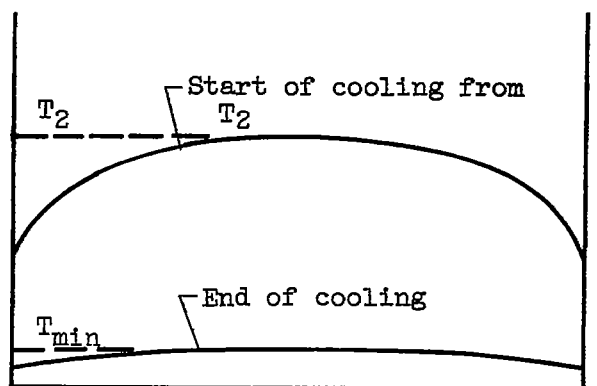
Distance along length of test section

(b) Cooling from $T_{max} = T_2 < T_1$.

Figure 9. - Temperature conditions during cooling.

4669

CE-6
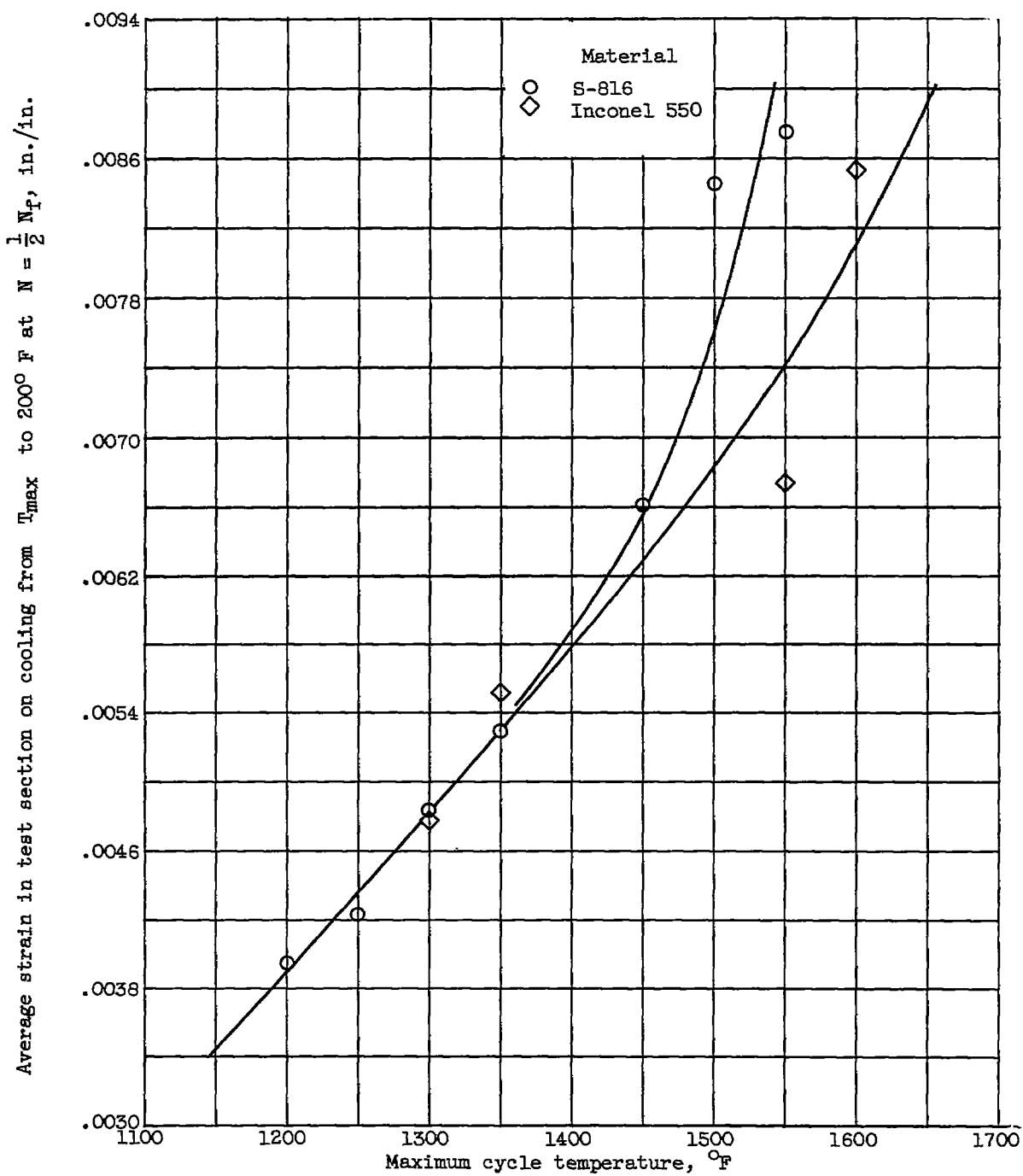
(a) Average strain.

Figure 10. - Stress change and average strain in test section during con-
strained cooling from various maximum cycle temperatures to a minimum
cycle temperature of 200° F at $N = \frac{1}{2} N_f$.
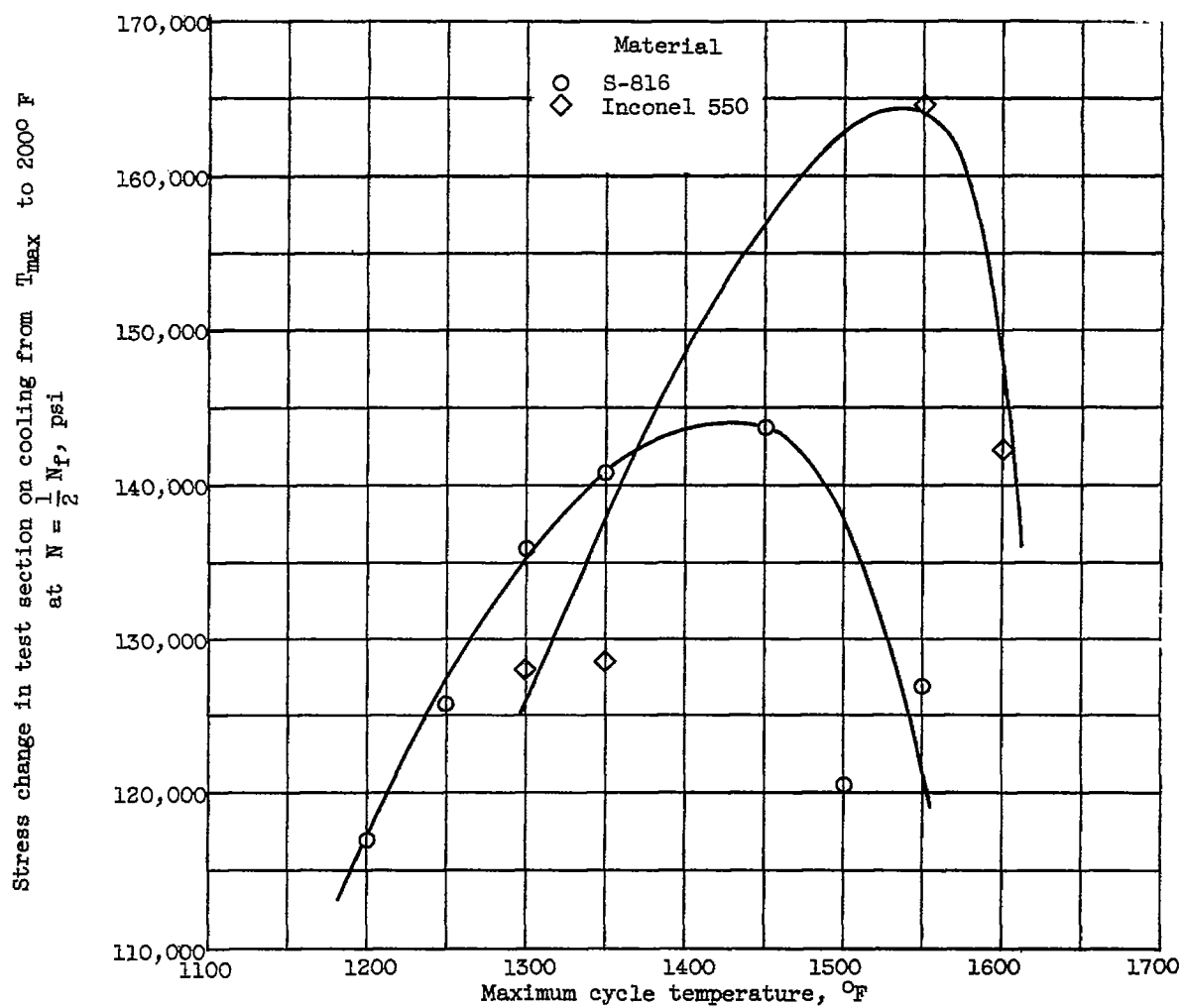
(b) Stress change.

Figure 10. - Concluded. Stress change and average strain in test section during constrained cooling from various maximum cycle temperatures to a minimum cycle temperature of 200° F at $N = \frac{1}{2} N_f$.
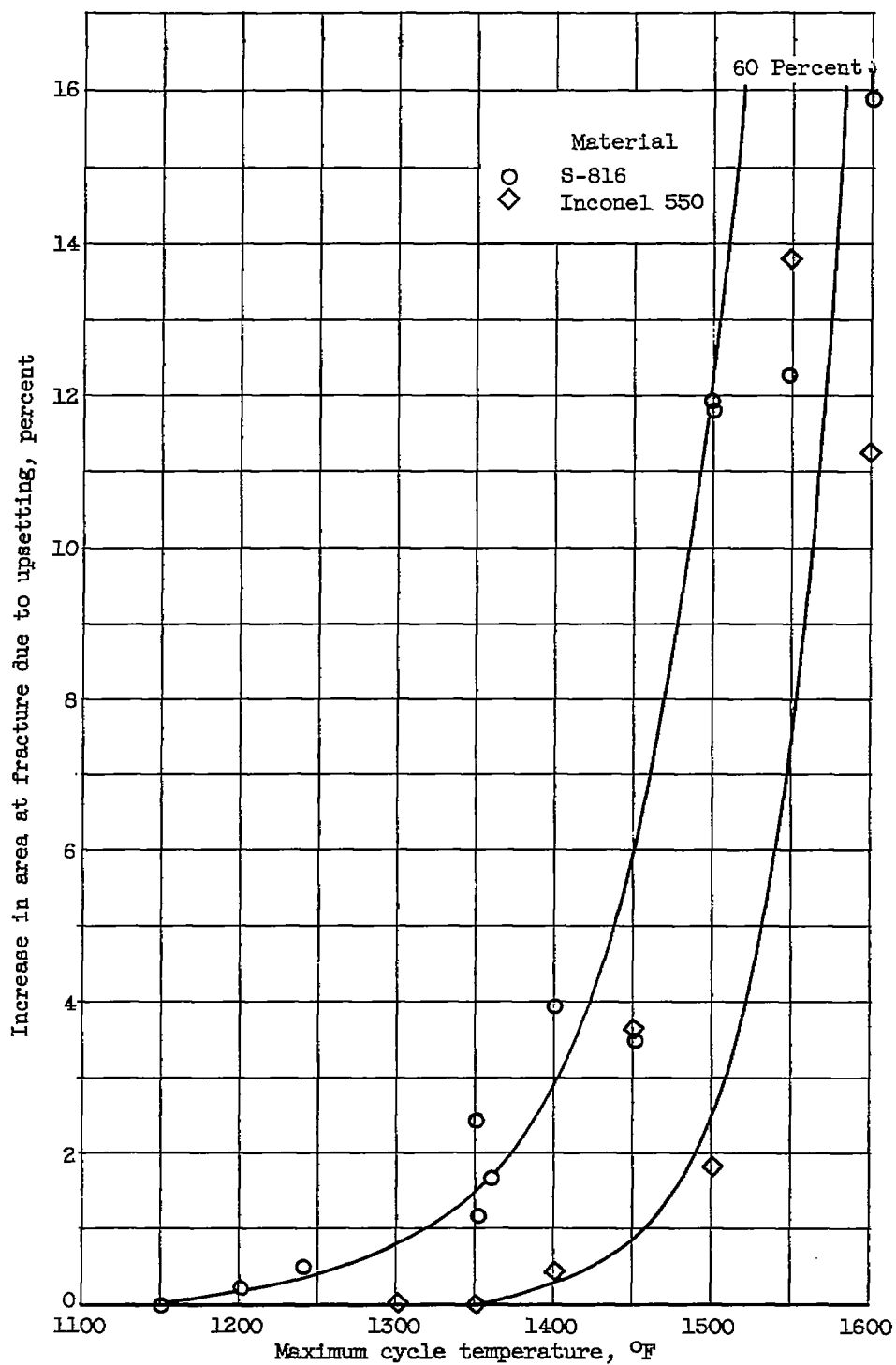
Figure 11. - Amount of bulging in specimens that had failed
in thermal fatigue at various T_{max}. Minimum cycle tempera-
ture, 200° F; clamped at maximum cycle temperature; heat or cool,
30 seconds; at temperature, 15 seconds.
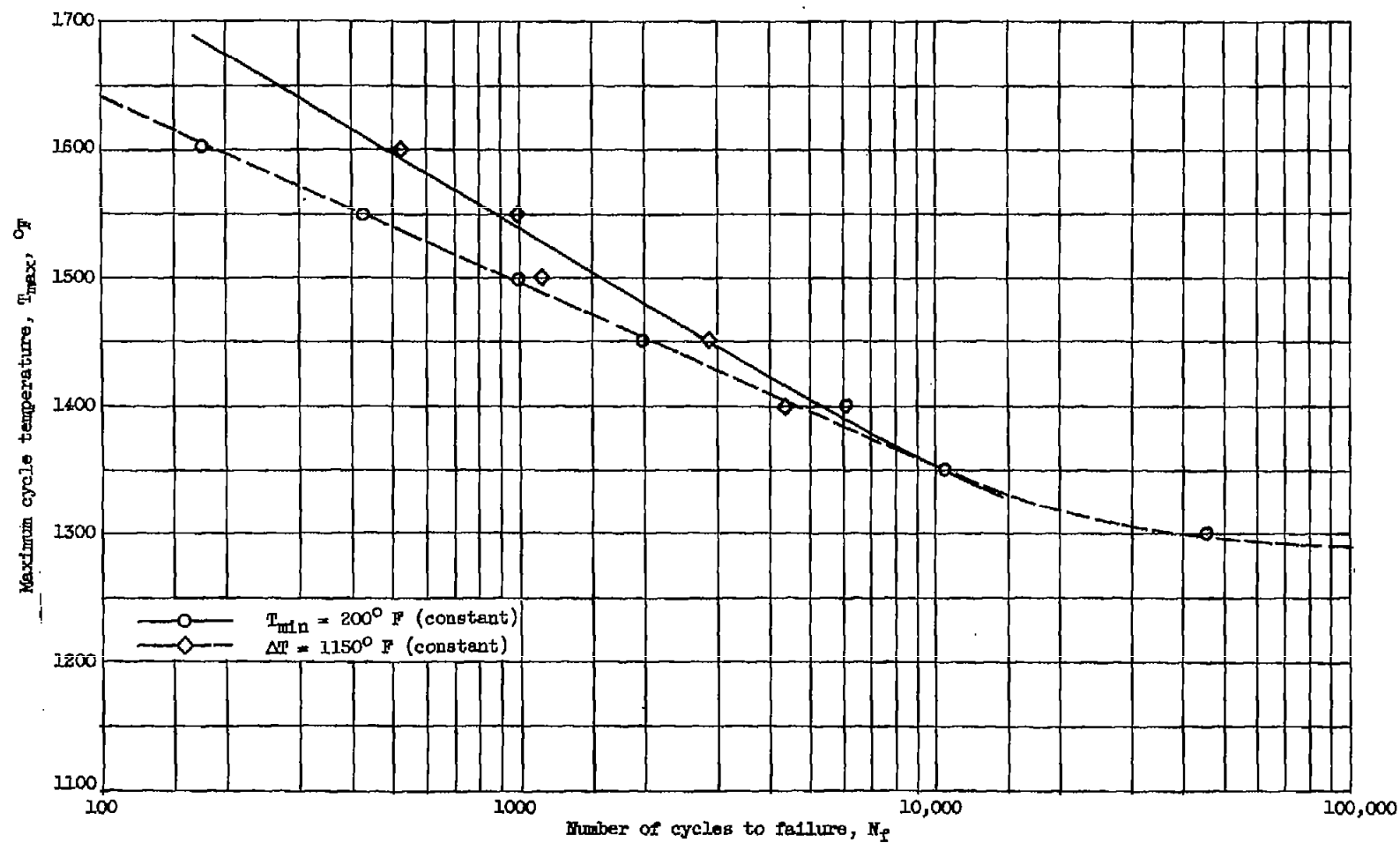
(a) For Inconel 550 specimens.

Figure 12. - Effect of T_{max} on N_f for specimens thermally cycled at a constant ΔT and at a constant T_{min}. Heat or cool, 30 seconds; at temperature, 15 seconds.
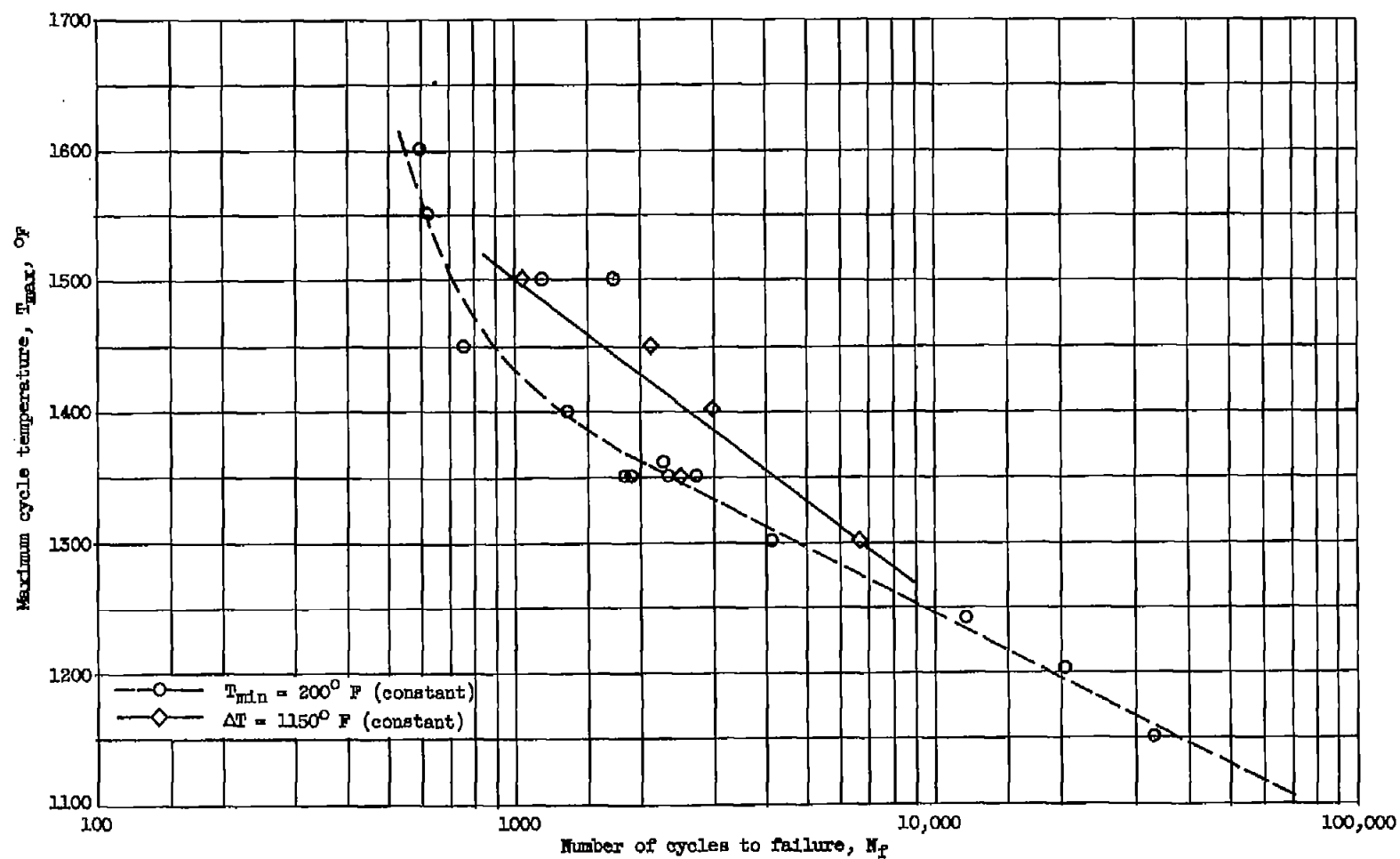
(b) For S-816 specimens.

Figure 12. - Concluded. Effect of T_{max} on N_f for specimens thermally cycled at a constant ΔT and at a constant T_{min}. Heat or cool, 30 seconds; at temperature, 15 seconds.
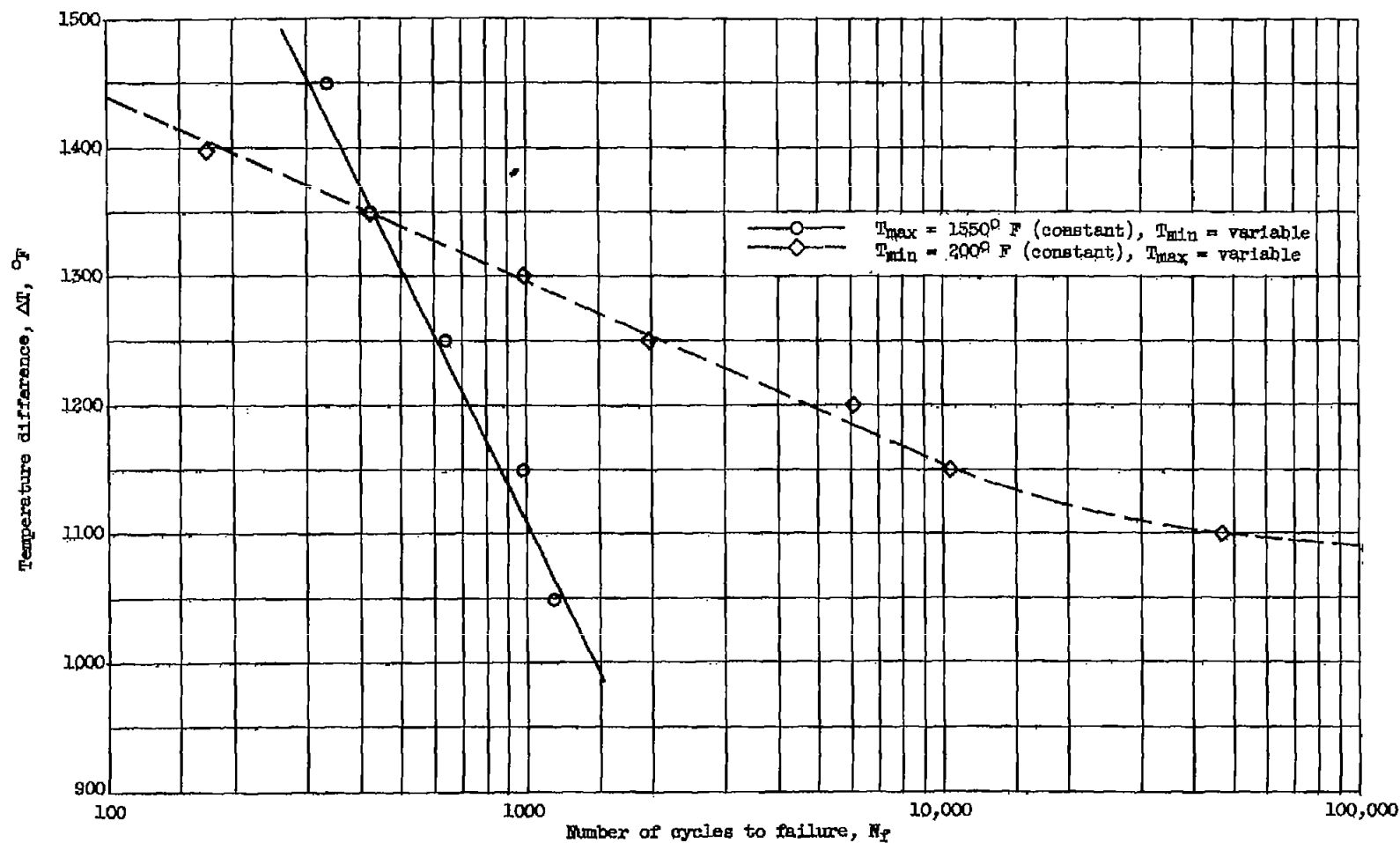
Figure 13. - Effect of ΔT on N_f for Inconel 550 specimens thermally cycled at a constant T_{max} and at a constant T_{min}. Heat or cool, 30 seconds; at temperature, 15 seconds.
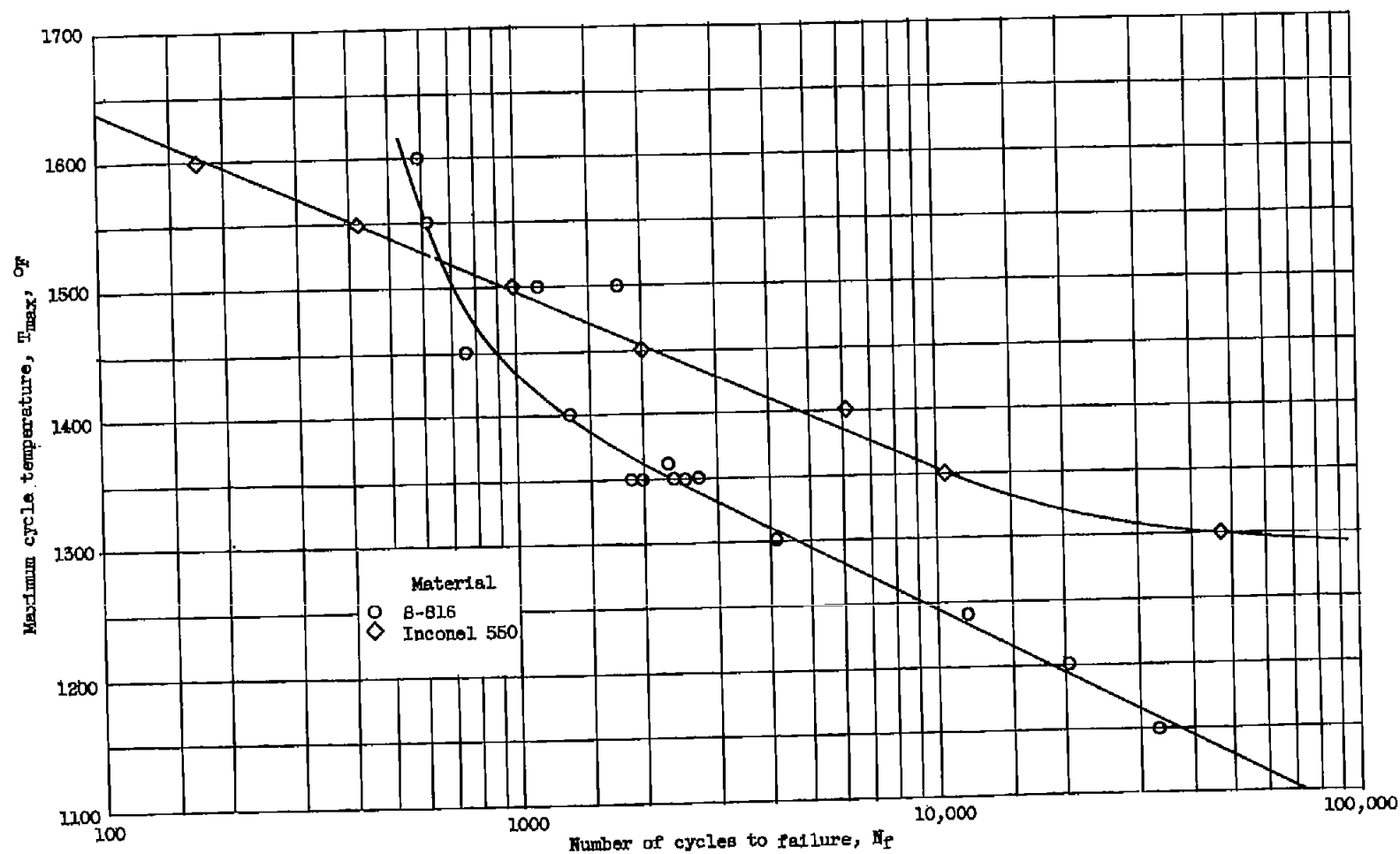
Figure 14. - Effect of T_{max} on N_f for S-816 and Inconel 550 specimens thermally cycled at a constant T_{min}. Minimum cycle temperature, 200° F; heat or cool, 30 seconds; at temperature, 15 seconds.
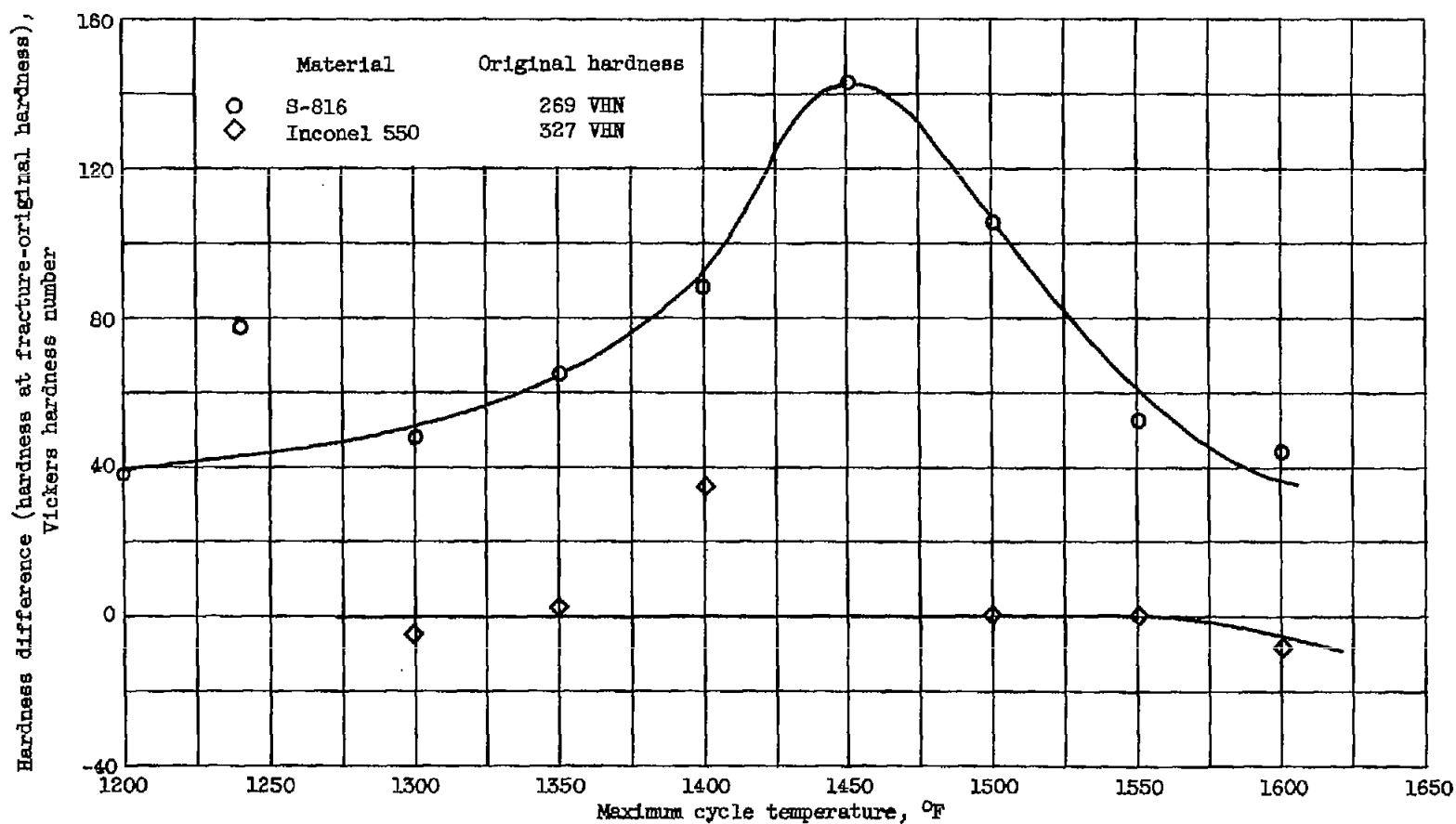
Figure 15. - Effect of T_{max} on the amount of hardness change of S-816 and Inconel 550 specimens that had been fractured as a result of thermal fatigue. Minimum cycle temperature, 200° F; heat or cool, 30 seconds; at temperature, 15 seconds.
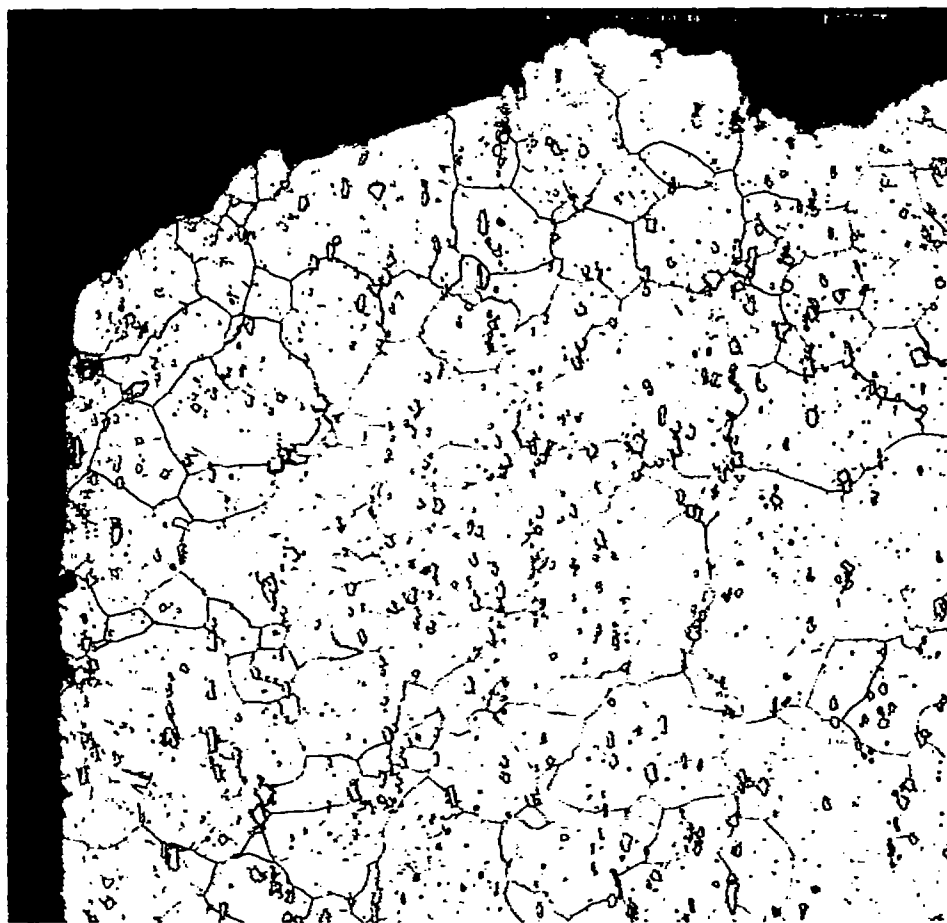
C-48026

(a) S-816 specimen fractured between 1200° and 200° F. Electrolytically etched in a solution of aqua regia and glycerol. X250.

Figure 16. - Microstructure of specimen that had been fractured by thermal fatigue.
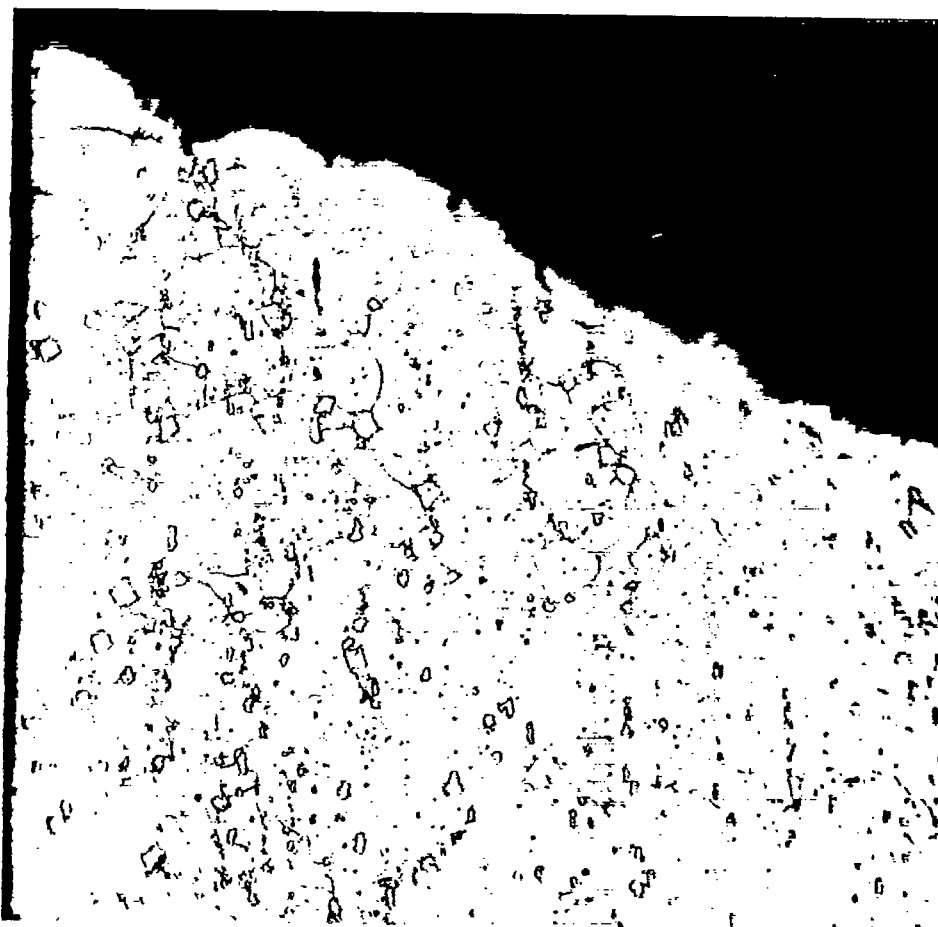
C-48027

(b) S-816 specimen fractured between 1450° and 200° F. Electrolyt-
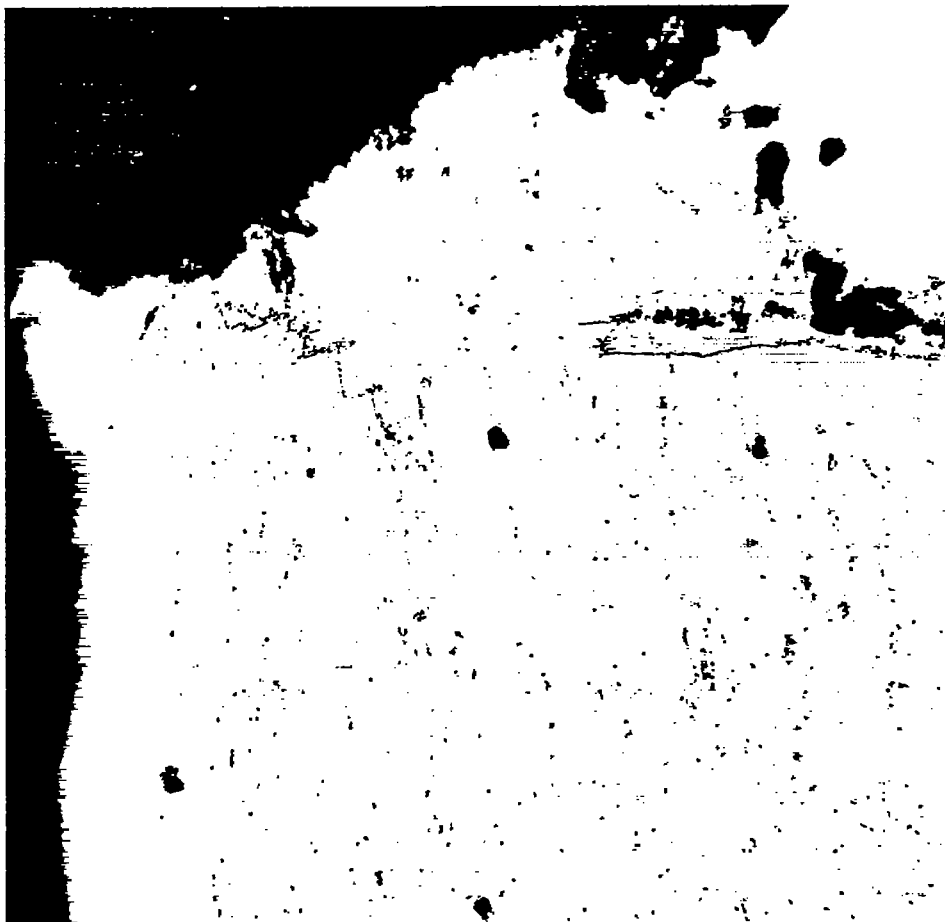   ically etched in a solution of aqua regia and glycerol. X250.

Figure 16. - Continued. Microstructure of specimen that had been
    fractured by thermal fatigue.
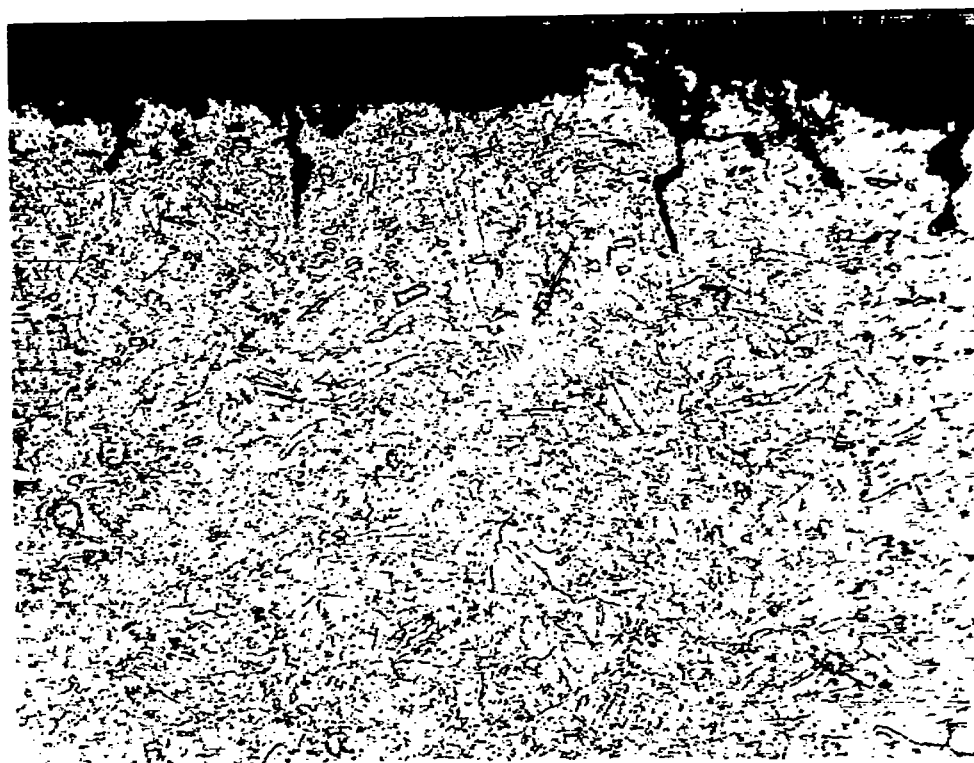
C-48028

(c) S-816 specimen fractured between 1600° and 200° F. Electrolytically etched in a solution of aqua regia and glycerol. X250.

Figure 16. - Continued. Microstructure of specimen that had been fractured by thermal fatigue.

C-48029

(d) Inconel 550 specimen fractured between 1350° and 200° F.
Electrolytically etched in a solution of sulfuric acid,
aqua regia, and Marble's reagent. X250.

Figure 16. - Continued. Microstructure of specimen that had
been fractured by thermal fatigue.

C-48030

(e) Inconel 550 specimen fractured between 1550° and 200° F.
   Electrolytically etched in a solution of sulfuric acid,
   aqua regia, and Marble's reagent. X250.

Figure 16. - Continued. Microstructure of specimen that had
been fractured by thermal fatigue.

C-48031

(f) Inconel 550 specimen fractured between 1600° and 200° F.
Electrolytically etched in a solution of sulfuric acid,
aqua regia, and Marble's reagent. X250.

Figure 16. - Continued. Microstructure of specimen that had
been fractured by thermal fatigue.

4669

C-48032

(g) Inconel 550 specimen fractured between 1600° and 200° F.
Electrolytically etched in a dilute solution of hydrofluoric
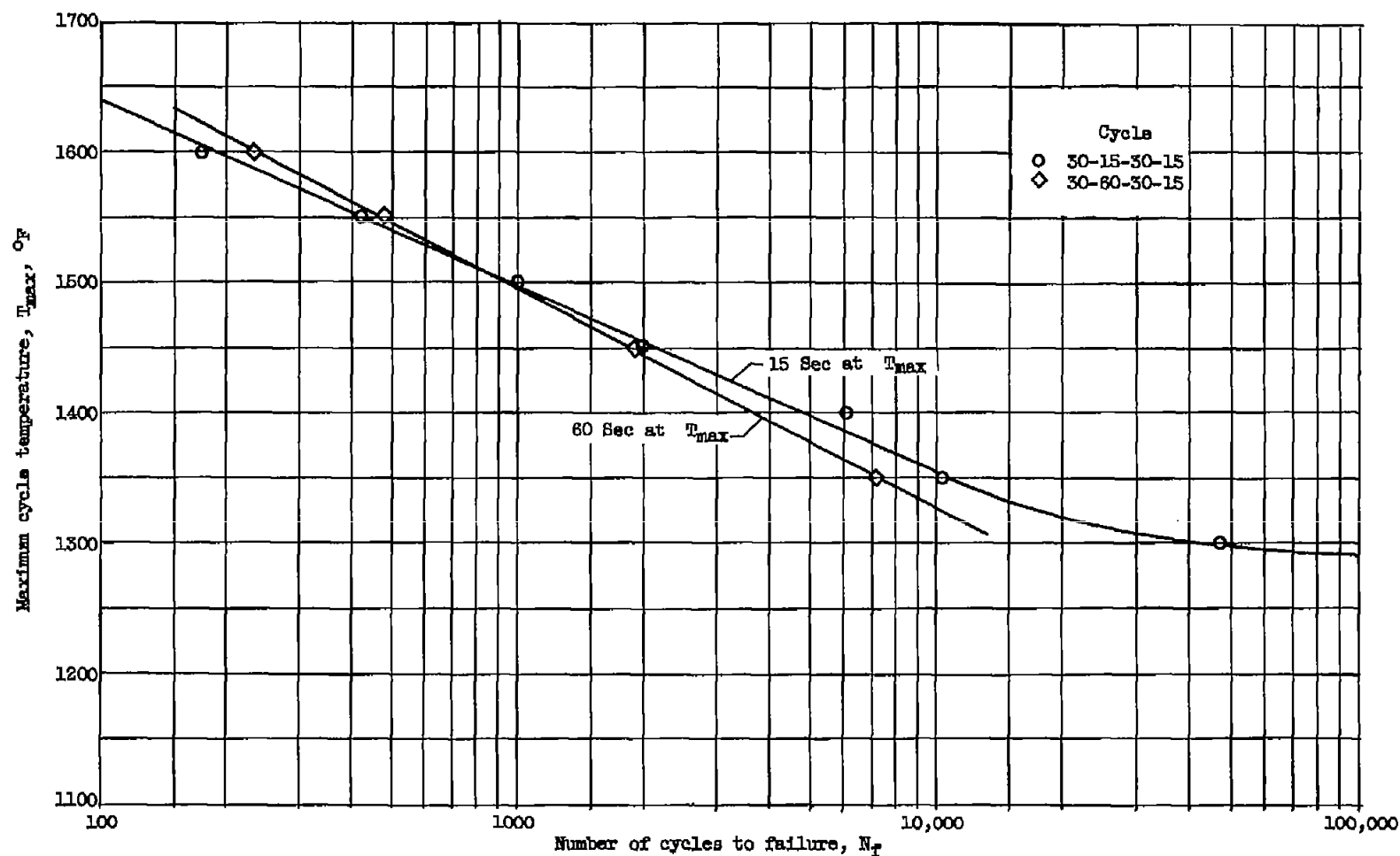acid and glycerol in water. X100.

Figure 16. - Continued. Microstructure of specimen that had
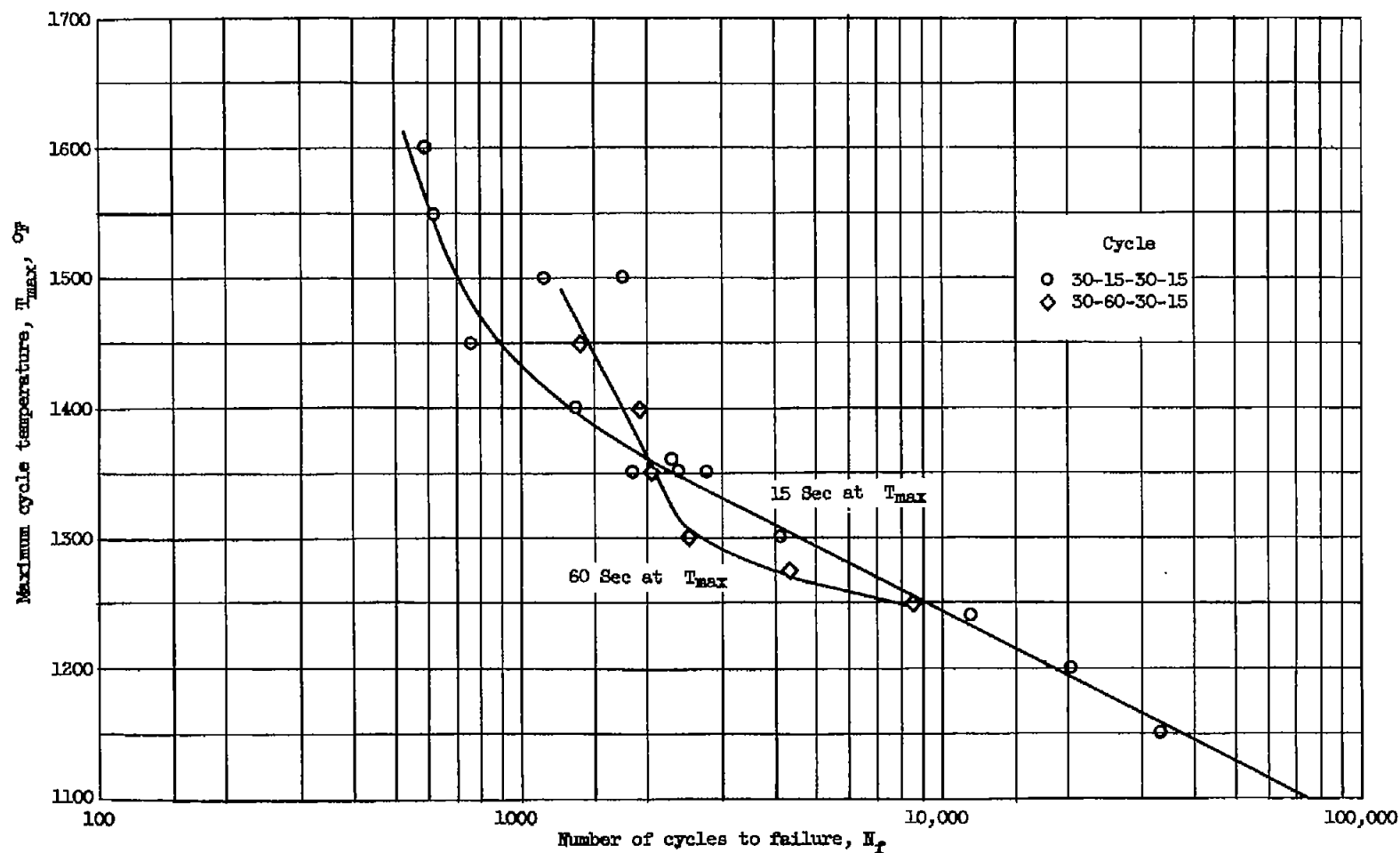been fractured by thermal fatigue.

C-48033

(h) Inconel 550 specimen fractured between 1600° and 200° F.
　　Electrolytically etched in a dilute solution of hydrofluoric
　　acid and glycerol in water.　X750.

Figure 16. - Concluded.　Microstructure of specimen that had
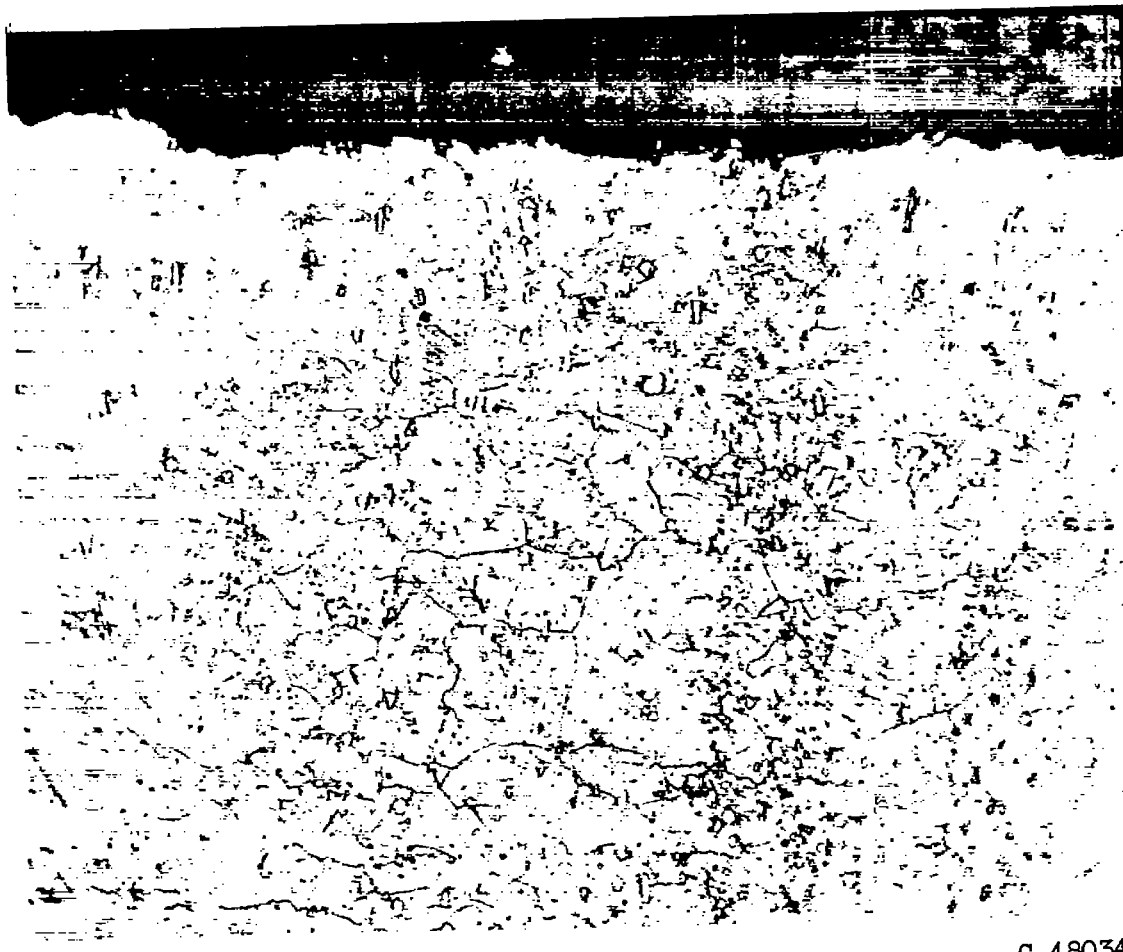　　been fractured by thermal fatigue.

(a) Inconel 550.

Figure 17. - Effect of time of exposure at T_{max} on N_f for specimens thermally cycled at various T_{max}. Minimum cycle temperature, 200° F.

(b) S-816.

Figure 17. – Concluded. Effect of time of exposure at T_{max} on N_f for specimens thermally cycled at various T_{max}. Minimum cycle temperature, 200° F.

4669

C-48034

(a) S-816 specimen fractured between 1250° and 200° F. Electrolytically etched in a dilute solution of sulfuric and boric acids.

Figure 18. - Microstructure of specimen that had been fractured by thermal fatigue on 30-60-30-15 cycle. X250.

C-48035

(b) Inconel 550 specimen fractured between 1350° and 200° F. Electrolytically etched in a solution of hydrochloric, nitric, and sulfuric acids.

Figure 18. - Concluded. Microstructure of specimen that had been fractured by thermal fatigue on 30-60-30-15 cycle. X250.
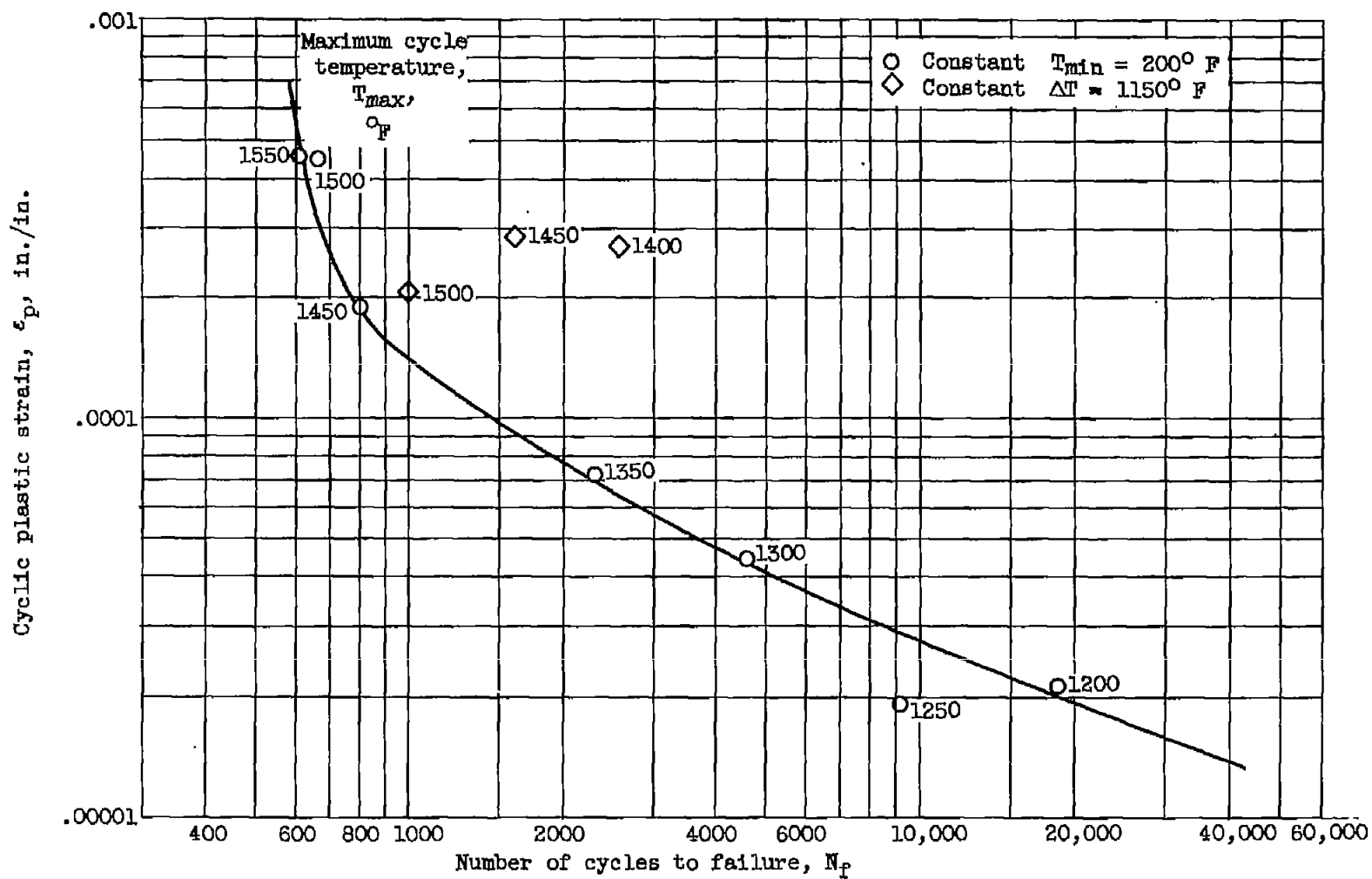
Figure 19. - Variation of the number of cycles to failure of S-816 specimens with the average plastic strain per half cycle. Heat or cool, 30 seconds; at temperature, 15 seconds.